UNCLASSIFIED
SECURITY CLASSIFICATION OF THIS PAGE

AD-A210 269

ELECTE JUN 21 1989 H

REPORT DOCUMENTATION PAGE

1a. REPORT SECURITY CLASSIFICATION: Unclassified	1b. RESTRICTIVE MARKINGS
2a. SECURITY CLASSIFICATION AUTHORITY	3. DISTRIBUTION/AVAILABILITY OF REPORT: Approved for public release; distribution unlimited.
2b. DECLASSIFICATION/DOWNGRADING SCHEDULE	
4. PERFORMING ORGANIZATION REPORT NUMBER(S)	5. MONITORING ORGANIZATION REPORT NUMBER(S): ARO 23736.1-EL
6a. NAME OF PERFORMING ORGANIZATION: UNIVERSITY OF SOUTHERN CALIF. / 6b. OFFICE SYMBOL (If applicable)	7a. NAME OF MONITORING ORGANIZATION: U. S. Army Research Office
6c. ADDRESS (City, State, and ZIP Code): LOS ANGELES, CA 90089-0241	7b. ADDRESS (City, State, and ZIP Code): P. O. Box 12211, Research Triangle Park, NC 27709-2211
8a. NAME OF FUNDING/SPONSORING ORGANIZATION: U. S. Army Research Office / 8b. OFFICE SYMBOL (If applicable)	9. PROCUREMENT INSTRUMENT IDENTIFICATION NUMBER: DAAL03-86-K-0102
8c. ADDRESS (City, State, and ZIP Code): P. O. Box 12211, Research Triangle Park, NC 27709-2211	10. SOURCE OF FUNDING NUMBERS: PROGRAM ELEMENT NO. / PROJECT NO. / TASK NO. / WORK UNIT ACCESSION NO.

11. TITLE (Include Security Classification) Experimental Investigations of Transport and Optical Properties of III-V Quantum Well Structures Grown Via Molecular Beam Epitaxy under Optimal Growth Conditions.

12. PERSONAL AUTHOR(S): A. MADHUKAR

13a. TYPE OF REPORT	13b. TIME COVERED	14. DATE OF REPORT (Year, Month, Day)	15. PAGE COUNT
PROGRESS	FROM 01/01/87 TO 12/31/88	1989, Apr. 18	53

16. SUPPLEMENTARY NOTATION The view, opinions and/or findings contained in this report are those of the author(s) and should not be construed as an official Department of the Army position, policy, or decision, unless so designated by other documentation.

17. COSATI CODES		
FIELD	GROUP	SUB-GROUP

18. SUBJECT TERMS (Continue on reverse if necessary and identify by block number) Mobility Inverted Hemt, Square Quantum Wells, Interface Disorder and Band Edge Discontinuity Fluctuations, Photoluminescence, Coupled Double Quantum Wells & Light Modulation, (cont'd p.11)

19. ABSTRACT (Continue on reverse if necessary and identify by block number)

Zero field mobilities in GaAs/$Al_xGa_{1-x}As$(100) inverted HEMT structures in excess of 10^5 cm^2/V-Sec at LN_2 temperatures have been achieved. The possibility of high mobilities in square single quantum wells with modulation doping on the inverted interface side only is demonstrated. Photoluminescences linewidth (Γ_{PL}) dependence on the square single quantum well width (d_w) shows $\Gamma_{PL} \sim d_w^{-1}$ rather than the $\Gamma_{PL} \sim d_w^{-3}$ behavior expected from the popularly used notion of well width fluctuations. The observed behavior is shown to be consistent with fluctuations in the band edge discontinuity (i.e. well depth) arising from in-plane fluctuations in the alloy composition of the $Al_xGa_{1-x}As$ barrier layers in high quality structures. Influence of an electric field across single and coupled-double quantum wells on their optical characteristics is examined theroretically and through photoluminescence, photocurrent, electroreflectance, photoreflectance and Photovoltage measurements. An amplitude modulation of 5 for an applied bias of 1.2 V across a 0.8 μm thick CDQW structures at 77 K has been formed, indicating struc-/..

20. DISTRIBUTION/AVAILABILITY OF ABSTRACT	21. ABSTRACT SECURITY CLASSIFICATION	
☐ UNCLASSIFIED/UNLIMITED ☐ SAME AS RPT. ☐ DTIC USERS	Unclassified	
22a. NAME OF RESPONSIBLE INDIVIDUAL	22b. TELEPHONE (Include Area Code)	22c. OFFICE SYMBOL

DD FORM 1473, 84 MAR — 83 APR edition may be used until exhausted. All other editions are obsolete.

SECURITY CLASSIFICATION OF THIS PAGE
UNCLASSIFIED

18.Cont'd.: Laser Assisted GaAs on Si, Quantum Wells on Patterned GaAs Substrates, Quantum Wells, Resonant Tunnelling, Quantum Magneto Transport and Cyclotron Resonance.

19. Abstract -(Cont'd from Page 10)

tures to be better suited for spatial light modulator structures than repeated single quantum wells exploiting the quantum confined Stark effect. GaAs/$Al_xGa_{1-x}As$ quantum well structures were grown on patterned GaAs (100) substrates and examined via photoluminescence (and electron microscopy). Exploiting growth conditions controlled thermodynamic and kinetic effects on facet formation and inter-facet migration, a unique in-situ method for realization of quantum wire and quantum box structures without the need for lithography or direct-write patterning on such small dimensions is demonstrated. Finally, some initial results on resonant tunneling diodes are reported. Realization of LN_2 (dark) mobilities of $\sim$ 150,000 cm^2/V-Sec in I-HEMT structures with carrier concentration 2-4 x $10^{10}/cm^2$ is reported. Such remarkably high mobilites at extremely low carrier concentrations open the way for quantum magneto-transport measurements relating to the fractional quantum Hall effect in regimes of Landau filling factor (ν) down to values of order 1/30 for fields up to 55T. Such work is under progress.

ARO 23736.1-EL

PROGRESS REPORT

(a) Title of Project:
Experimental Investigations of Transport and Optical Properties of III-V Quantum Well Structures Grown Via Molecular Beam Epitaxy under Optimal Growth Conditions

(b) Name of Institution:
Department of Materials Science and Engineering
University of Southern California
Los Angeles, CA 90089-0241

(c) Period Covered by Report: Jan. 1, 1987 - Dec. 31, 1988

(d) ARO Project Number: P-23736-EL

(e) Contract Number: DAAL03-86-K-0102

(f) Author(s) of Report: A. Madhukar

(g) Personnel Supported: P.51

PROGRESS REPORT

ON

CONTRACT # DAAL 03-86-K-0102

ARMY RESEARCH OFFICE
RESEARCH TRIANGLE PARK
P.O.BOX 12211
NORTH CAROLINA, 27709-2211

ATTN.: DR. M. STROSCIO

PERIOD COVERED: JAN. 1, 1987 - DEC. 31, 1988

SUBMITTED BY: A. MADHUKAR
DEPARTMENT OF MATERIALS SCIENCE
UNIVERSITY OF SOUTHERN CALIFORNIA
LOS ANGELES, CA 90089-0241

TABLE OF CONTENTS

		Page No.
	PREAMBLE	2
I.	WORK ACCOMPLISHED	2
	A. TRANSPORT IN HETEROJUNCTIONS AND SQUARE QUANTUM WELLS	2
	B. OPTICAL PROPERTIES OF ALLOYS AND SQUARE QUANTUM WELLS	8
	C. THE QUANTUM CONFINED STARK EFFECT	17
	D. COUPLED-DOUBLE QUANTUM WELLS	18
	E. LASER-ASSISTED AND NON-ASSISTED GaAs ON Si(100)	27
	F. PHOTOLUMINESCENCE FROM WELLS GROWN ON PATTERNED SUBSTRATES	33
	G. QUANTUM WIRE STRUCTURES	38
II.	WORK IN PROGRESS	41
	A. VERTICAL TRANSPORT	41
	B. MAGNETO-QUANTUM TRANSPORT	44
	C. CYCLOTRON RESONANCE	46
	D. ABSORPTION IN COUPLED-DOUBLE QUANTUM WELLS	46
III.	PUBLICATIONS	49
IV.	STUDENTS/POST-DOCS TRAINED	51
V.	COLLABORATIONS/INTERACTIONS	52

PREAMBLE:

These pages contain a progress report on the work accomplished and various activities undertaken during the period Jan. 1, 1987 to Dec. 31, 1988 under Contract No. DAAL 03-86-K-0102. The report is divided into two main sections. Section I covers work accomplished while section II covers a status report of work under progress. Section III provides a list of publications either solely or partially supported by this contract, section IV a list of personnel, and section V a brief description of collaborative interactions.

I. WORK ACCOMPLISHED:

In this section we provide a brief description of some of the salient accomplishments to date under the present contract. The work accomplished is grouped under different headings which are indicative of the generic theme.

(I.A) TRANSPORT IN HETEROJUNCTIONS AND SQUARE QUANTUM WELLS:

During the period Jan. '87 - Jan. '88 we focussed on certain outstanding experimental and theoretical issues relating to electron transport parallel to the interfaces in heterojunctions (HJ's) and square quantum wells (SQW). In the former category we focussed on the inverted high electron mobility transistor (I-HEMT) whereas, as is the latter category, we focussed on the single SQW.

THE I-HEMT

Through usage of the growth and surface smoothness recovery kinetics of GaAs(100) and $Al_xGa_{1-x}As(100)$ growth fronts extracted from our RHEED studies during MBE, we arrived at an optimized approach to growing I-HEMT structures which would maintain high quality inverted interface in spite of usage of very low (500-550°C) growth temperature during modulation doping of $Al_{0.25}Ga_{0.75}As$. The notion of growth interruption was employed with the novel twist of delivering $\leq$ 1 ML of GaAs periodically during $Al_{0.25}Ga_{0.75}As$ growth prior to growth interruption. Comparison of the inverted HEMT's grown (during 1986) on our O-400 MBE machine following conventional approach and our new approach showed an increase in mobility by a factor of 5 to 7 but the absolute values were still limited to - 22,000 Cm^2/V-Sec. This was clearly attributable to the lack of adequate background vacuum conditions of this old machine as revealed by high carbon and other impurity related luminescence. The correctness of the basic idea being, however, demonstrated by the results, we initiated a collaboration with colleagues at the US Army Electronics and Device Technology Laboratory, Ft. Monmouth, to grow the I-HEMT structures following our approach on their high quality Varian GenII MBE machine. The very first set of I-HEMT grown showed LN_2 mobilities in the dark between 80,000 and 90,000 Cm^2/V-Sec for carrier concentrations of - $5\text{-}7x10^{11}/Cm^2$. Mobilities under light were as high as ~125,000Cm^2/V-Sec. These remarkably high mobilities (a factor of 5 better than those previously reported

without the use of superlattice buffer layers) established the correctness of the ideas and demonstrated, for the first time, that I-HEMT mobilities can be made comparable to the normal HEMT's. Further details may be found in publications nos. 9,10 and 11 of the publication list given in sec. III.

Since our new RIBER 3200P MBE system was delivered and became operational in Fall 1988, we have succeeded in obtaining unheard of LN_2 dark mobilities of 145,000 to 150,000 Cm^2/V-Sec in I-HEMT structures with the remarkably low electron density of $\sim 3 \times 10^{10}/Cm^2$. Although such low density electron gas is of no particular significance to any conventional electronic de-vice, the greater achievement here is the realization of such high mobilities at such low densities - a much sought after objective for basic Physics studies and one at which previous attempts by many have been unsuccessful. Such electron gases are suited for both, examination of transport and magneto-transport characteristics in a regime of electron density previously not available (along with high mobility) and possible examination of new electron-electron interaction dominated phenomenon at very low temperatures ($\leq$ mk) and very high magnetic fields ($\geq$ 35T). This regime includes such things as charge density wave and possibly quantum Wigner solid formation, apart from the integral and fractional quantum Hall effects. Work on these aspects is presently underway and we discuss it at the end of this section.

SINGLE SQUARE QUANTUM WELL:

In parallel with the I-HEMT effort noted above, we undertook both theoretical and experimental work on the behavior of electron mobility in single square quantum wells (SSQW) of GaAs/$Al_{0.3}Ga_{0.7}As$ as a function of well width (d_w), spacer layer thickness (d_{sp}), single side modulation doping (inverted and normal) and carrier concentration. We developed self-consistent solutions for coupled Schrodinger and Poisson equations accounting for the electron-electron exchange and correlation effects within the X approximation. The resulting self-consistent bound state energies, wave functions, and charge density distribution were employed to examine the role of remote ionized impurity, alloy disorder and band edge discontinuity fluctuation induced scattering employing the memory function approach based on the Kubo formalism. The results showed that the low temperature mobilities in ~200A wide wells can be as high as 4 to 5 $x10^6$ Cm^2/V-Sec. though for normal side modulation doped SSQW this is about a factor of 2 smaller than the highest mobilities possible in N-HEMT. A number of other interesting predictions also came out of these calculations, discussed in publication nos. 4 and 5.

On the experimental side a large number of SSQW's were grown with varying structural and/or doping schemes, including δ-doping. Their Hall mobility behavior was systematically examined as a function of temperature (4K to 300K). The predicted factor of 2 difference between the N-HEMT and SSQW was confirmed although the absolute value for the latter was limited to 52,000 Cm^2/V-Sec

(a) NORMAL STRUCTURE

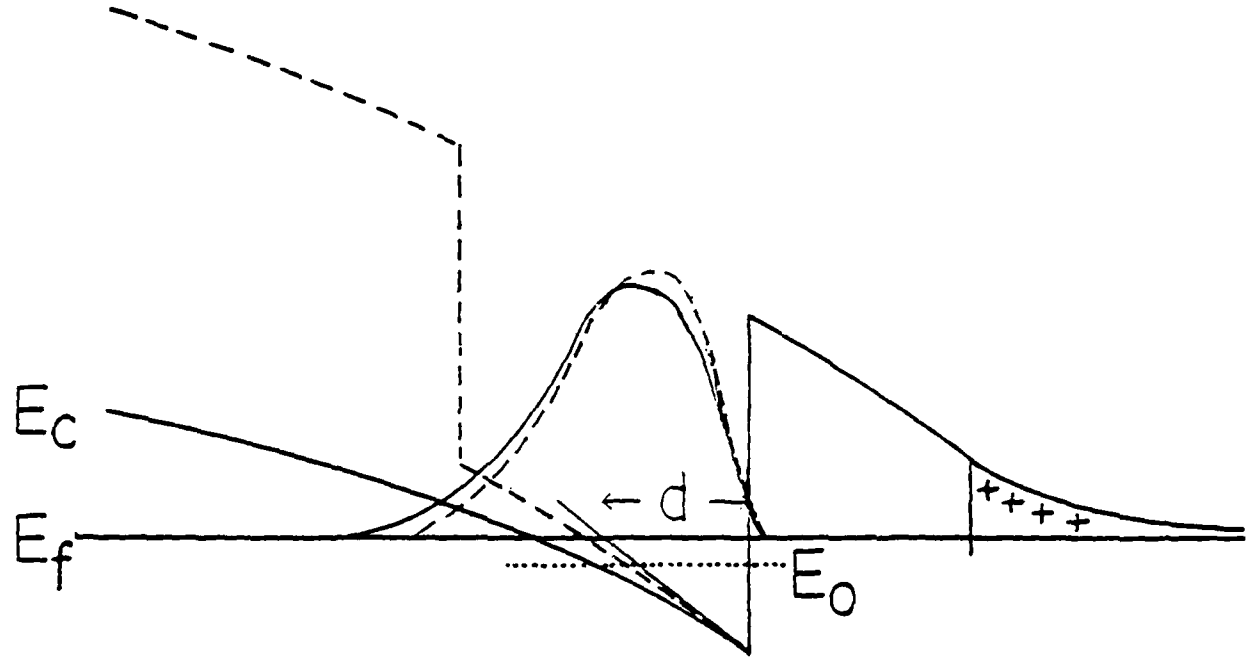

surface →

(b) INVERTED STRUCTURE

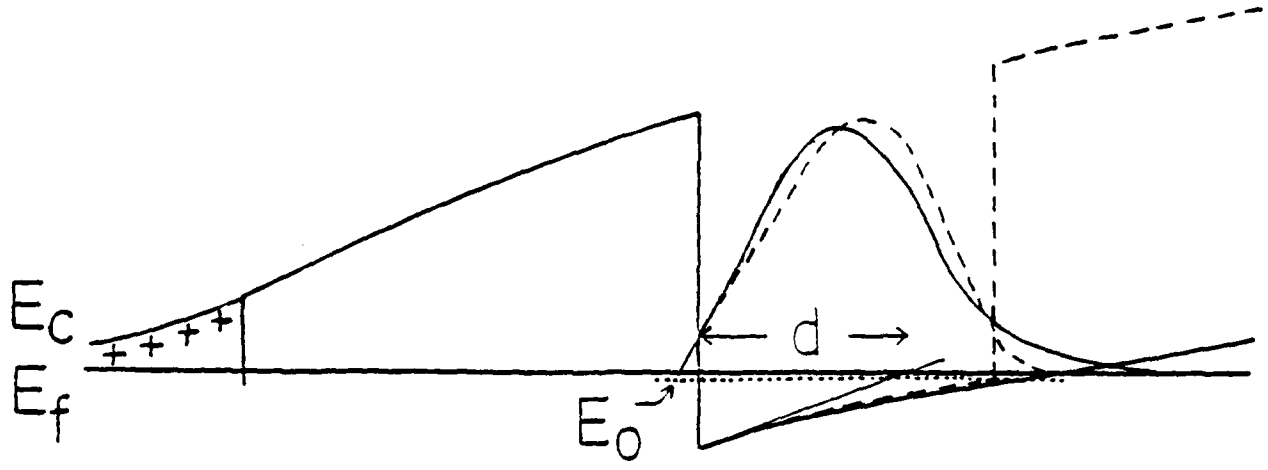

Fig. 1

at LN_2 temperature. This was directly attributable to the less than necessary ambient quality of our O-400 MBE machine and we have no doubt that, just as in the case of I-HEMT discussed above, growth in high quality machines is fully capable to improving the SSQW mobilities by at least the same factor of 5 as found for I-HEMT's, if not even more. We are presently examining this aspect via growth on our new RIBER 3200P MBE system.

A very interesting result which has emerged from the studies so far is the first umambiguous identification of the influence of the inverted interface induced scattering in SSQW. Since this work has just been submitted for publication, we note here the salient findings. Introduction of a square well in the normal HJ was found to decrease the mobility by a factor of two whereas for the inverted structure the mobility was found to increase by a factor of two. This unexpected latter result is shown to be a consequence of the shifting of the confined carrier charge distribution away from the inverted interface due to a self-consistent change in band bending as schematically represented in fig. 1 (panel (a) for the normal and panel (b) for the inverted structure). This has led to the recognition that in an inverted structure the absolute mobility of the SSQW can be even higher than the I-HEMT if one is already in the regime where the I-HEMT mobility is limited by the inverted interface scattering rather than remote ion scattering. This is not possible in the normal structure, thus indicating that the I-SSQW (and not I-HEMT) can have mobilities as high as the N-HEMT. Further details may be

found in publication no. 17 of sec. III.

(I.B) OPTICAL PROPERTIES OF ALLOYS AND SQUARE QUANTUM WELLS:

During the present reporting period, a wide range of experimental and theoretical studies relating to the optical behavior of GaAs/$Al_xGa_{1-x}As$ based quantum well structures were undertaken. The primary experimental techniques employed were,

Near Band Edge Photoluminescence (PL)

Photoluminescence Excitation Spectroscopy (PLE)

Raman Scattering (RS)

Rayleigh Scattering (RLS)

Electro-Reflectance Spectroscopy (ERS)

Photo-Reflectance Spectroscopy (PRS).

In the following we provide a brief description of some of the more important findings of these experimental studies, some of which address basic issues of the optical properties of relevance to quantum wells and others which address the basic nature of the $Al_xGa_{1-x}As$ alloy barrier layer itself - an aspect which influences the nature of the quantum well but had not been carefully and systematically examined prior to our studies. First, however, we note some theoretical studies which played a critical role in dileneating the TRUE ATOMISTIC NATURE of the interfaces defining the confining potential in quantum wells.

THE PL LINE WIDTH DEPENDENCE ON WELL WIDTH:

Through a systematic examination of the low temperature (4K

to 40K) PL and PLE excitonic line widths as a function of well width in single square quantum wells of $GaAs/Al_{0.3}Ga_{0.7}As$ grown under identical and RHEED optimized growth conditions, we had found (see fig. 2) that $\Gamma_{PL} \propto d_w^{-1}$ rather than $\Gamma_{PL} \propto d_w^{-3}$ as predicted by the prevalent notion that it is the well width fluctuation which is the line width determining factor. This popular notion and model having been ruled out by our experimental findings, we were naturally faced with the task of finding out what gave rise to the observed $\Gamma_{PL} \propto d_w^{-1}$ behavior. (We note the same is true of $_{PLE}$ and for both Γ_{PL} and Γ_{PLE} the same was found to hold up to temperatures as high as 40K).

Based upon our computer simulations of MBE growth of GaAs/$Al_xGa_{1-x}As$ quantum wells (undertaken under ONR sponsorship) we had already identified the presence of in-plane Al composition fluctuations (i.e. along the interfaces) arising from the differences in the Al and Ga migration and reaction kinetics. Such fluctuations from the intended global composition were found to occur on length scales of 20 to 100A, depending upon the growth kinetics operative under the chosen growth conditions. Thus it was clear to us that the exciton size in the quantum wells being of order 100A (radius), the recombination life time must be influenced by the presence of such local Al concentration fluctuations i.e. fluctuations in the band-edge discontinuity (the depth of the confining potential). Thus under the present ARO Grant we undertook development of a theory of the PL linewidth due to exciton scattering by (a) the band-edge discontinuity

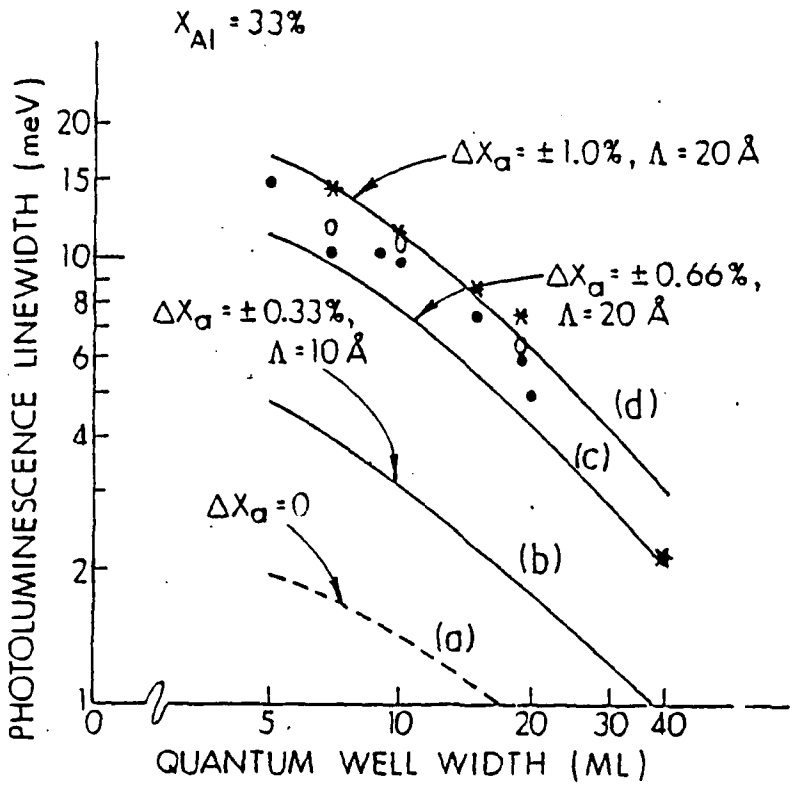

The measured dependence of the PL linewidth on the quantum-well width d_w. Solid circles and asterisks indicate data taken at 5 K and 40 K, respectively. The open circles are linewidths determined in PL excitation spectra taken at 5 K. The dashed line corresponds to the theory, retaining only the microscopic alloy-disorder contribution, while the solid lines correspond to the results obtained with inclusion of varying degrees of composition fluctuation of amplitude ΔX_a and correlation length Λ.

FIGURE 2

fluctuations, and (b) alloy disorder experienced by the exciton due to its wave function penetrating into the alloy barrier layers. The local Al concentration (on the scale of the exciton size) fluctuation correlation function was modelled as a Gaussian. The calculated line width as a function of well width showed the observed nearly d_w^{-1} dependence, in conformity with the experimental findings. It is perhaps worth noting that, subsequently, Ourzmad et.al.[1] through transmission electron microscope lattice imaging and image simulation studies determined the existence of such Al concentration fluctuations on the length scales of 20-50A, in conformity with our computer simulation findings, as well as substantiating our physical model for the observed $\Gamma_{PL} - d_w^{-1}$ behavior.

This work is to be found in publication no. 1 of the list of publications given in section (III).

DOUBLE-RESONANCE RAMAN AND OPTICAL PHONON - ELECTRON RESONANT MIXING:

Nearly a decade ago, we predicted[2] a resonant mixing between the two quasi two dimensionally confined electronic states when their separation becomes comparable to an optical phonon energy. Early experimental efforts to observe this phenomena were based on making the cyclotron resonance frequency in a two dimensional electron gas comparable to the optical phonon energy. While some indication of the existence of the phenomena was found in dc measurements (the so-called magnetophonon effect) in

$GaAs/Al_{0.3}Ga_{0.7}As$ HJ's and in ac measurements in the InAs/GaSb HJ's, the results could not provide as clear and direct information as could be obtained due to the lack of high enough magnetic fields and electron screening effects. Consequently, we devised the appropriate $GaAs/Al_{0.3}Ga_{0.7}As$ SQW structure consisting of 8 or 9 ML wide GaAs well, undoped, for which the light hole (lh) and heavy hole (hh) separation is close to the GaAs bulk LO phonon frequency of ~36 meV. Then, under the resonant excitation condition of $h\nu_{inc} \doteq (lh \rightarrow e^-)$, the outgoing single phonon Raman photon satisfies $h\nu_{out} = (hh \rightarrow e^-)$, thus creating a DOUBLE RESONANCE condition, enhancing Raman cross section dramatically. Consequently, in the secondary emission spectra we observed the double Resonance Raman Scattering (DRRS) lines corresponding to three optical phonons, along with the usual photo luminescence. In the PL excitation spectra (a sort of analog of absorption), a remarkable 27 peaks were observed riding over the step-like quasi 2D density of states (see fig. 3). These peaks were shown to correspond to a radical modification of the 2D density of states due to resonant mixing of 16 different optical phonons of the SQW structure with the light and heavy hole states. These 16 phonons were shown to belong to the categories of confined in the well, confined in the barrier, interface, and unconfined phonon states of a square quantum well structure. This is, and remains, the only simultaneous observation of all possible phonon states of a SQW structure, apart from providing a clear and unambiguous confirmation of our theoretical predictions. Details may be found

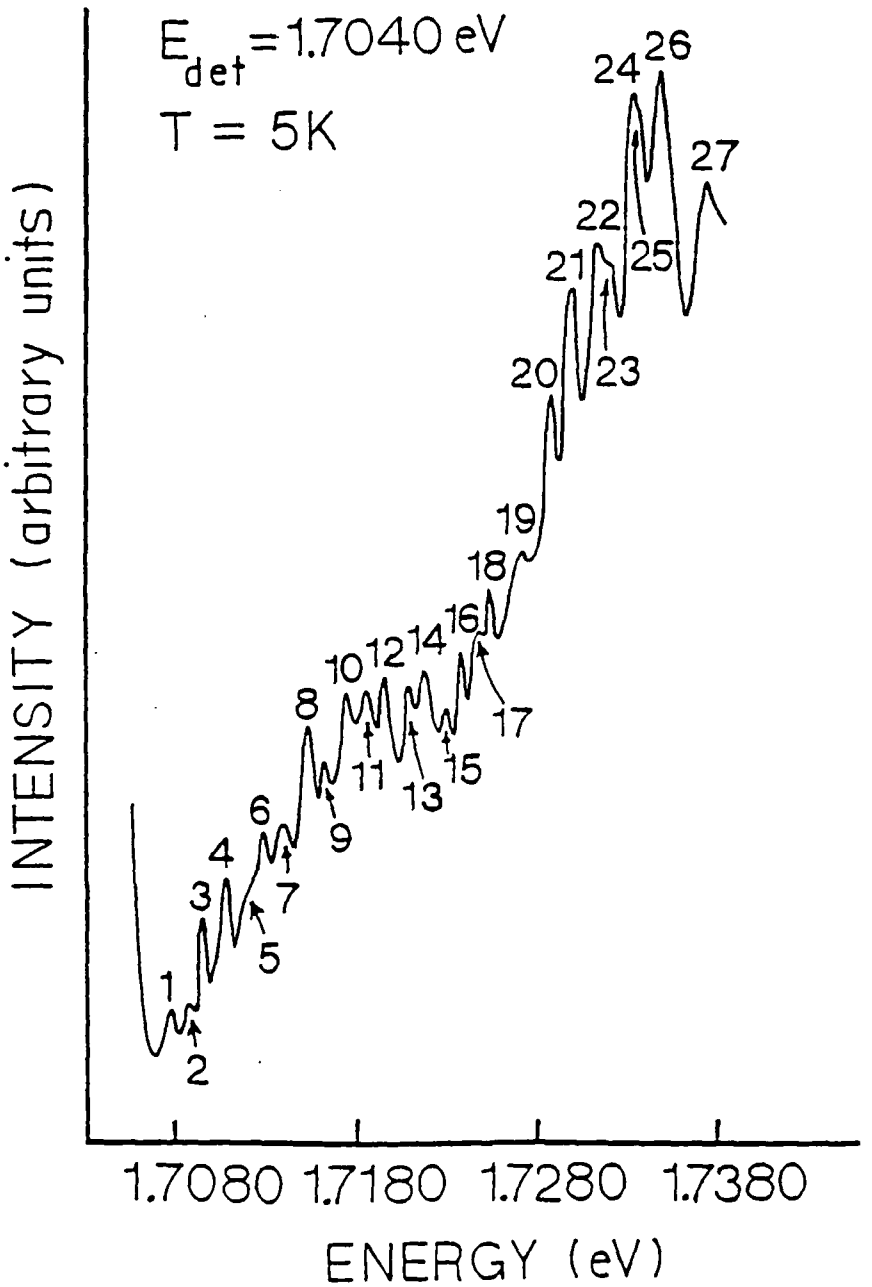
E det = 1.7040 eV
T = 5K
INTENSITY (arbitrary units)
1
2
3
4
5
6
7
8
9
10
11
12
13
14
15
16
17
18
19
20
21
22
23
24
25
26
27
1.7080
1.7180
1.7280
1.7380
ENERGY (eV)

Fig. 3

in publication nos. 4 and 7.

POLARIZATION BEHAVIOR OF EXCITONIC RECOMBINATION IN SQW'S:

Although the polarization behavior of bulk semiconductors (such as GaAs) has been shown to provide useful information on the momentum and energy relaxation of the photoexicted carriers, studies of the polarization behavior of excitonic recombination in confined structures had not been undertaken prior to our studies. We examined this behavior for both, ordinary SQW structures and the double resonance SQW structure discussed in the preceding. The orinary SQW structures exhibited little or no linear polarization. The double resonance SQW's, on the other hand, showed a strong linear polarization dependence on the incident photon energy. They also showed a reduction in the PL linewidth. These effects were attributable to the strong modification of the confined heavy hole level due to the resonant mixing with the light hole level brought about by the optical phonon. Details are to be found in publication no. 13.

COMBINED RAMAN, RAYLEIGH SCATTERING AND PHOTOLUMINESCENCE STUDIES OF $Al_xGa_{1-x}As$ ALLOYS:

Although the $Al_xGa_{1-x}As$ alloy is an integral part of the GaAs/$Al_xGa_{1-x}As$ system, most commonly employed for creation and study of heterojunctions and square quantum wells, its properties have not been investigated in a systematic way. Indeed our experimental RHEED studies during growth of $Al_xGa_{1-x}As$ alloys and

alloy barrier layers, as well as our Monte Carlo computer simulation studies had indicated that the quality of the alloy layer grown and the atomistic structural and chemical nature of the interfaces formed in quantum well structures must depend upon the kinetics of growth. The successful realization of the high mobilities in the I-HEMT structures discussed in section (I.A) was achieved by manipulating the kinetics based upon these realizations. We therefore undertook an optical investigation as well as an independent means of examining the correlation between tge RHEED and the growth kinetics in an effort to further strengthen the value of RHEED in arriving at optimized growth conditions for realization of high quality alloy layers and quantum well structures.

Systematic Raman scattering and Rayleigh scattering studies of thick $Al_{0.3}Ga_{0.7}As$ alloy layers grown under RHEED indicated optimized and non-optimized conditions were thus undertaken. The combination makes a powerful tool since while Raman scattering is sensitive to alloy disorder activated breakdown of selection rules, the Rayleigh scattering is sensitive to fluctuations in mass density that accompany defects and clustering effects. The studies clearly showed a significantly lower Rayleigh scattering in $Al_{0.3}Ga_{0.7}As$ alloys grown under RHEED optimized growth conditions as compared to samples grown under conditions indicated by the RHEED intensity dynamics to be non-optimal. Consistent with this, the Raman scattering showed significantly lawer intensity of disorder activated peaks and the absence of any bulk

GaAs-like peak in samples grown under RHEED optimized conditions. These studies thus constitute a direct optical determination of the power of RHEED in identifying optimized growth conditions.

The above noted approach was extended to examination of the quality of $Al_xGa_{1-x}As$ alloys as a function of the Al concentration (x). Note that the main point here is that the differences in the Ga and Al growth kinetics implies that the optimized growth conditions for alloys with differing x values are different. These studies were further supplemented by PL studies, thus gaining complimentary information on various length scales; atomic for Raman, of the order of the exciton size for PL, and long ranged for Raleigh scattering. At high Al concentrations (x- 0.8) we showed the occurrence of atomic scale (~10A) GaAs-like and AlAs-like regions in the sample. In addition, AlAs-like TO node was observed in the forbidden backscattering geometry and, unlike previous suggestions of alloy disorder effect, was attributed to twinning effects in the sample arising from strain effects and dependent upon the growth kinetics. The phonon-assisted excitonic recombination in the indirect band gap region (x>0.42) was, unlike earlier explanations, shown to involve phonon around the and L points as well, even though the dominant contribution arises from phonons around the X-point.

Another finding, of considerable pragmatic value and which comments on the common usage of PL and Raman scattering as a means of post-growth determination of alloy concentration, is that the prevalent expressions employed routinely for such interpretation

are not reliable to an accuracy better than $\pm$5%. In many cases, the discrepancy found within a given technique (PL or Raman) employing commonly used expressions (empirical or theoretical) for two different peaks is as large as 20%. A critical need for much more reliable theoretical expressions as well as empirical relations thus exists.

The details of these studies may be found in publication nos. 8, 12 and 15.

(I.C) THE QUANTUM CONFINED STARK EFFECT:

It has been shown that the application of an electric field across a square quantum well causes the excitonic absorption to shift to lower energy and a broadening of the absoprtion line width. This effect, dubbed the quantum confined Stark effect (QCSE) is a consequence of the shifting of the confined electron and hole wave functions away from each other due to the tilting of the quantum well potential under applied field. The QCSE is of some significance for it can be exploited for the creation of light amplitude modulation based spatial light modulators (SLM). It has been employed in a p-i-n configuration integrating the detection and modulation functions to create the self-electrooptic effect device (SEED)[3]. A basic limitation on the modulation depth achievable in devices based on the QCSE arises from the absorption broadening. Two basic mechanisms contribute to this broadening; (i) the broadening due to various departures from ideal quantu, well behavior present at zero and non-zero fields and (ii)

broadening arising from tunnelling if the applied field becomes large enough. The conventional model for the former nad been the usual well width fluctuation mechanism. However, as discussed in section (I.2), our PL experiments showed that the zero field line width is dominated by fluctuations in the band edge discontinuity and alloy disorder scattering. Consequently, we undertook a theoretical analysis of the influence of an electric field on the PL line width arising from these two dominant sources.

The PL line width was calculated as a function of applied field (0 to 100 KV/Cm) for varying well widths and barrier layer global alloy composition for the GaAs/$Al_xGa_{1-x}As$ SQW system. We showed that for a given well width (particularly >100A), the increase in line width with applied field is very sensitive to the degree of Al concentration fluctuations in the interface plane. The higher the amplitude of such fluctuation correlation function, the more rapid rapid the increase in the line width and hence, the less the absorption modulation. Thus once again, the control on the kinetics of growth through usage of optimized growth conditions is seen to be a key issue. Further details are to be found in publication no. 3.

(I.D) COUPLED-DOUBLE QUANTUM WELLS:

A coupled double quantum well (CDQW), shown schematically in fig. 4(a), gives rise to symmetric (S) and antisymmetic (AS) combinations of the individual isolated well states, the energy splitting being controlled by the width and height of the barrier

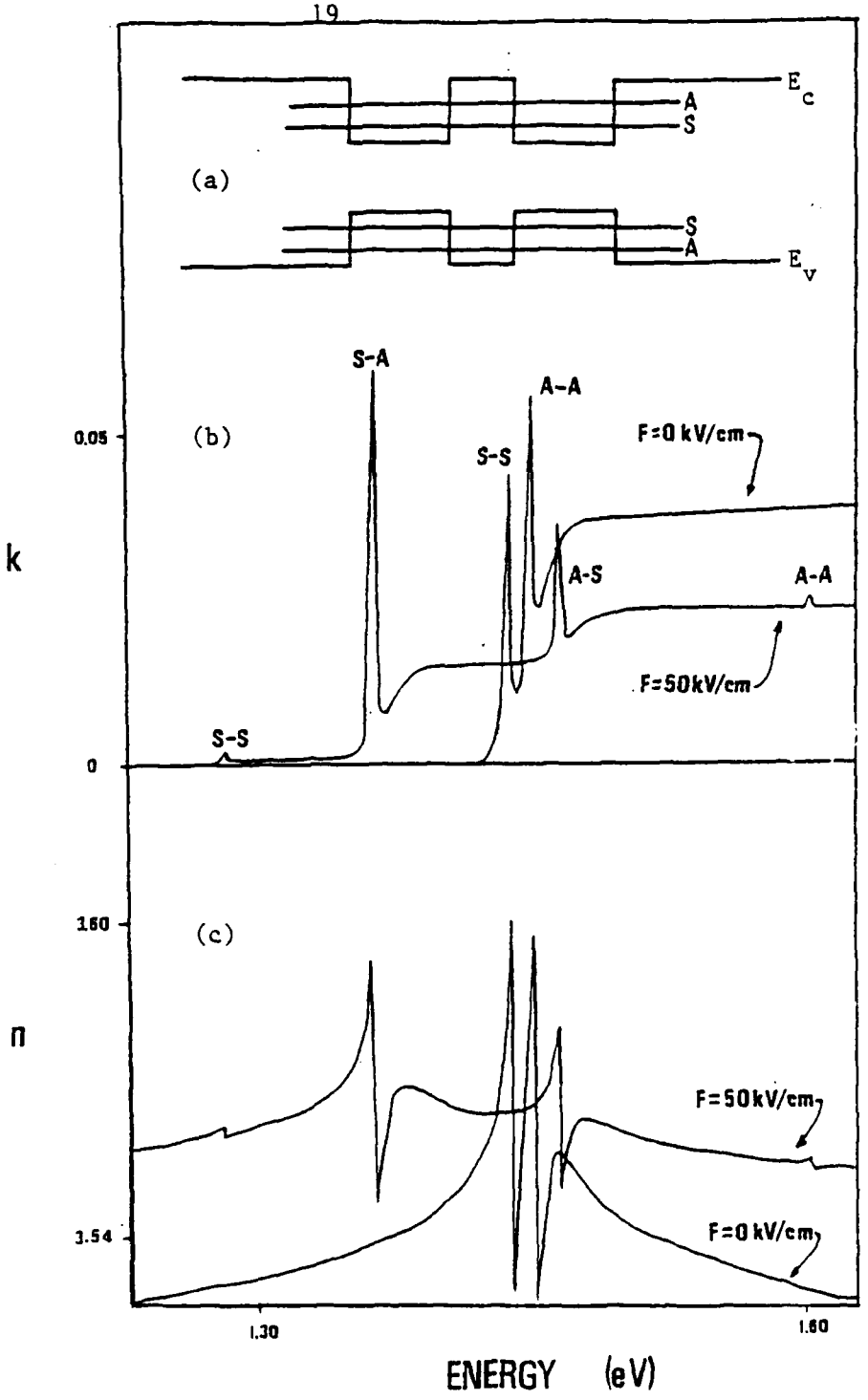

Fig. 4 (a) Shows schematic band diagram of CDQW under flat band conditions with the symmetric (S) and antisymmetric (A) confined electron and hole energy levels.
(b) Shows absorption coefficient k as a function of transition energy for 0 and 50 kV/cm total field based on phenomenological model.
(c) Shows index of refraction n as a function of transition energy for 0 and 50 kV/cm total field based on a phenomenological model.

layer. The electric dipole selection rules for absorption permit only S-S and AS-AS transitions under flat band conditions. Upon the application of an electric field, the tilting of the CDQW potential makes possible mixed transitions which gain oscillator strength at the expense of the S-S and AS-AS transitions. This physical process offers an interesting alternative to the QCSE for exploitation for achieving amplitude and/or phase modulation. Thus to gain a feel for the magnitude of changes in n and K we undertook calculations based upon a phenomenological approach which modelled the excitonic transitions as Lorentzian oscillators, the 2D density of states effect as a broadened step function, and the contribution of the unconfined states as a rising background. This lattermost contribution is essential to achieving a correct description of the underlying physics since even the behavior in the limited energy range of the confined states is dramatically influenced by all other states - a consequence of the fact that all states are eigenfunctions of the same Hamiltonian so that n and K in the confined state energy regime are significantly controlled, through the Kramers-Kronig relation, by their behavior at energies far away. An example of the calculated behavior for 40 ML GaAs wells coupled through a 5 ML wide $Al_{0.3}Ga_{0.7}As$ barrier layer is shown in fig. 4. One not only notices the build-up of the oscillator strengths in the transitions forbidden under flat band conditions, but also that at sufficiently large fields the AS heavy hole to S electron transition can be pulled below the band gap of the GaAs substrate.

Consequently, a large change in the absorption, going from the sub-band gap residual absorption ($\alpha<10Cm^{-1}$) to the high absorption ($\alpha\sim10^{4}Cm^{-1}$) at the mixed transition appears possible. Similarly, in other energy regime a significant change in n without a large change in K appears possible - a feature highly desirable for phase modulation based spatial light modulators.

Given the potential of CDQW, we undertook a systematic experimental study. Starting early '87, a large number of CDQW of varying well and barrier width were grown under RHEED optimized growth conditions on our O-400 MBE machine and their PL and PL excitation spectra examined as a function of applied bias. Two major experimental push-ups were necessary to undertake such a study. First, considerable effort went into optimizing the deposition conditions and thickness of the transparent metal gate - indium-tin oxide (ITO) along with the thickness of the $Al_{0.3}Ga_{0.7}As$ barrier layer immediately below so as to prevent damage to the CDQW structure during ITO deposition and to minimize ambiguities due to ITO induced strain effects in the CDQW. This part of the work was undertaken in collaboration with Prof. A.R. Tanguay, Jr. and his students with whom we evolved a collaborative effort on SLM's under the context of the URI on "Integration of Optical Computing" at USC. The second major push-up starting summer 1987 was in the area of setting up room temperature techniques such as electro-reflectance (ER) and photo-reflectance (PR). For the GaAs/AlGaAs based systems absorption measurements require etching of the backside substrate with a very high degree

of control and uniformity, while at the same time being careful about mechanical strain effects that may arise in a "free-standing" very thin film. Since absorption measurements are eventually the most direct and desirable measurements, a third effort begun in parallel was setting-up, at minimal cost, a home-built substrate chemical etching system in which the etching can be monitored via appropriate wavelength light transmission in real time. Setting up the ER and PR measurement systems also required resources not available under the present Grant. Nevertheless, by fall of '87 we established these facilities with some borrowed equipment, tested the measurement system against well known spectra for bulk GaAs and $Al_{0.3}Ga_{0.7}As$, optimized the system for signal to noise ratio and were finally ready by summer '88.

During '88 we have undertaken extensive studies of the CDQW structures employing PL, PLE, ER, PR, and photo-current (PC) spectroscopies. Some illustrative results are shown in fig. 5 (PC), fig. 6 (PL), fig. 7 (ER) and fig. 8 (comparison with theory). One clearly sees the influence of the applied field. A slight ambiguity that remains in such measurements relates to pin-pointing the exact condition under which the system is in flat-band condition - a consequence of the built-in field in grown structures due to the background doping and defects in the material. The cross checks provided by the simulataneous use of different techniques helps in this process. Work is presently continuing on optimizing this effect for SLM's.

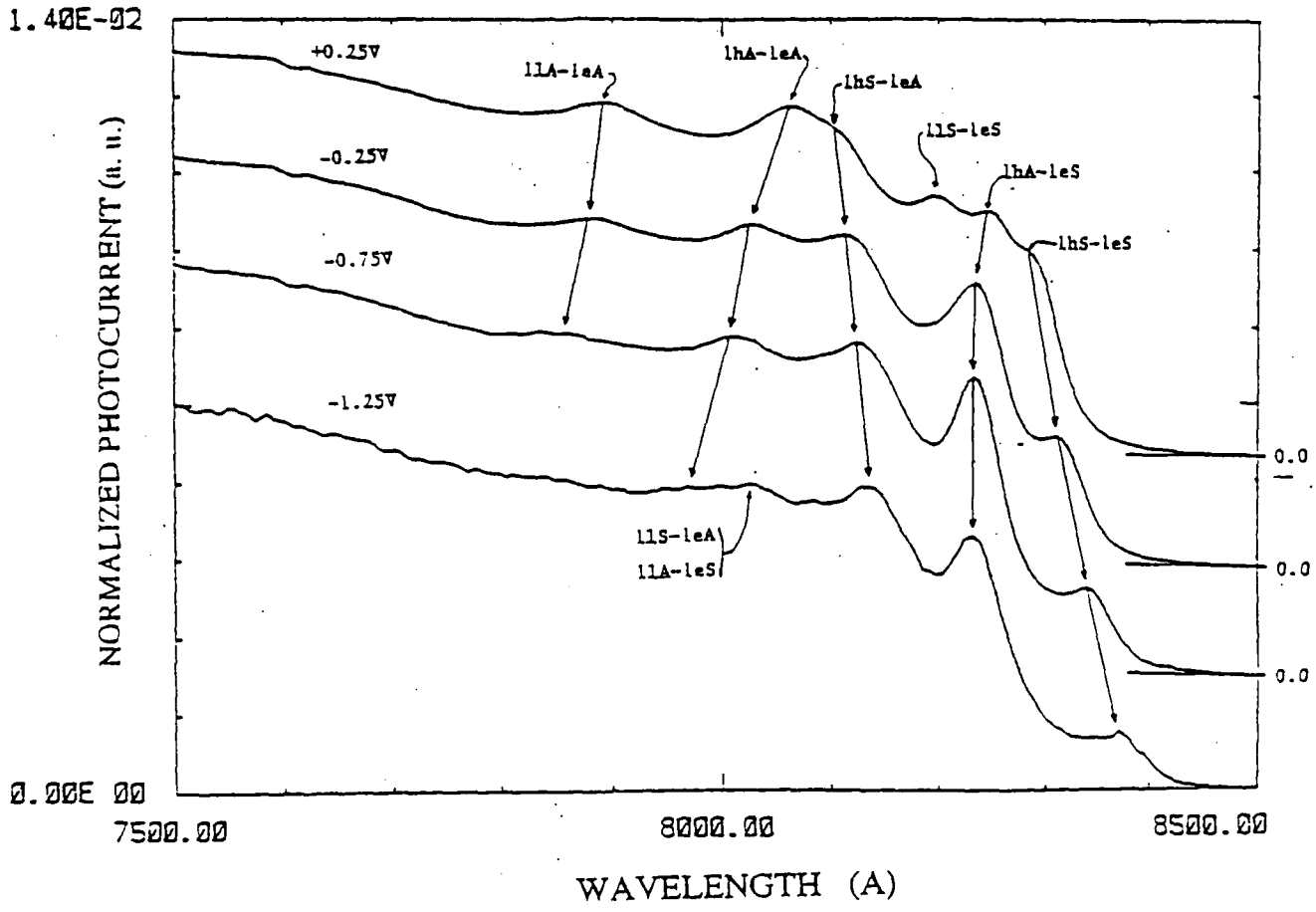

Fig. 5 Photocurrent spectra on a 20-5-20 monolayer CDQW with 20 pairs at room temperature for .25V (forward bias), and -.25V, -.75V, -1.25V (reverse bias). The total thickness of the CDQW region is 5208 A. The nomenclature of the assigned peaks are in the text. The zero level of each spectrum has been offset.

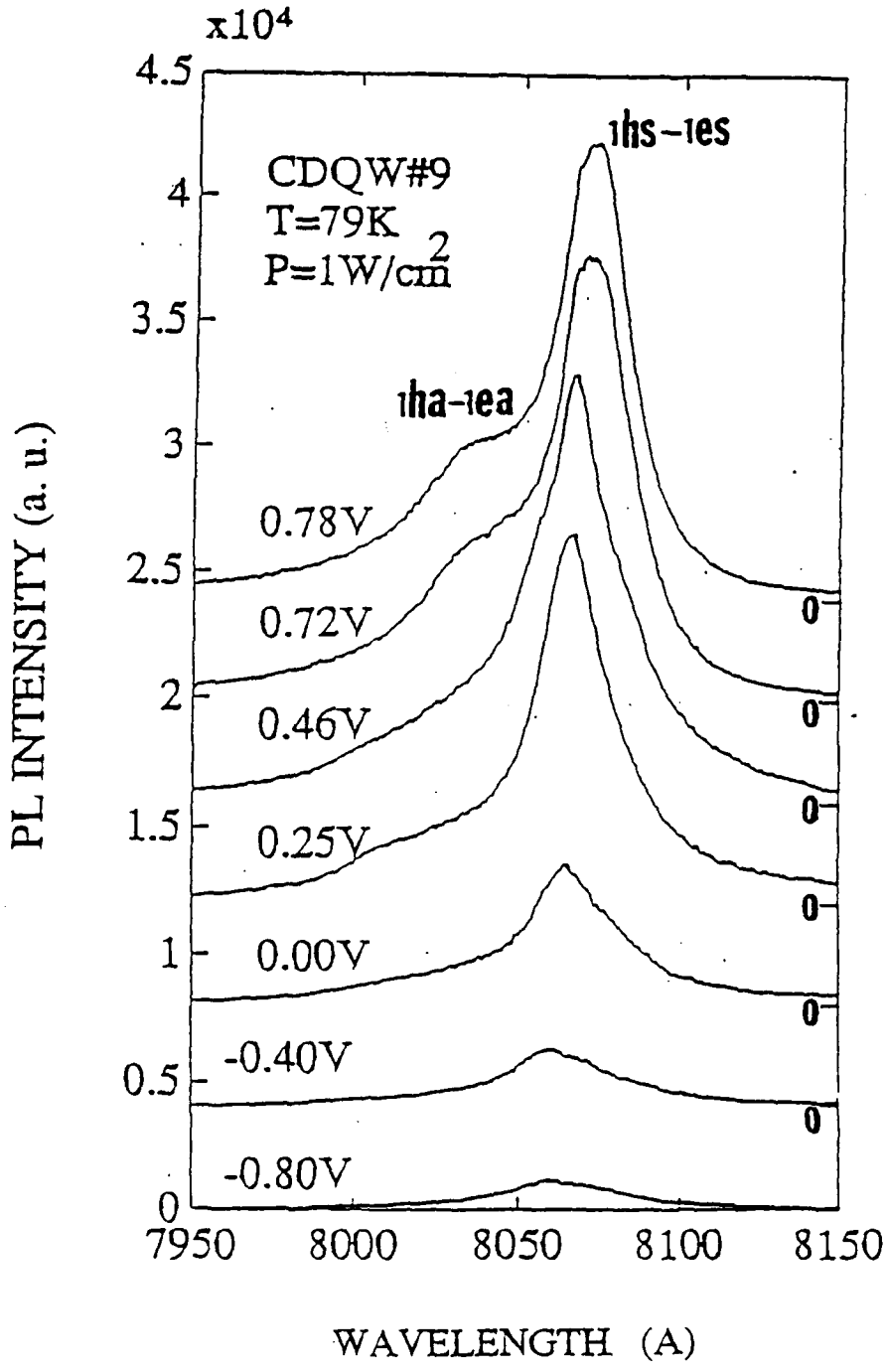

Fig. 6 Photoluminescence spectra on a 40-5-40 monolayer CDQW with 20 pairs at 79 K for 0.78V, 0.72V, 0.46V, 0.25V (forward bias), 0.0V, and -.4V, -.8V (reverse bias). The total thickness of the CDQW region is 7739 A. The zero level of each spectrum has been offset.

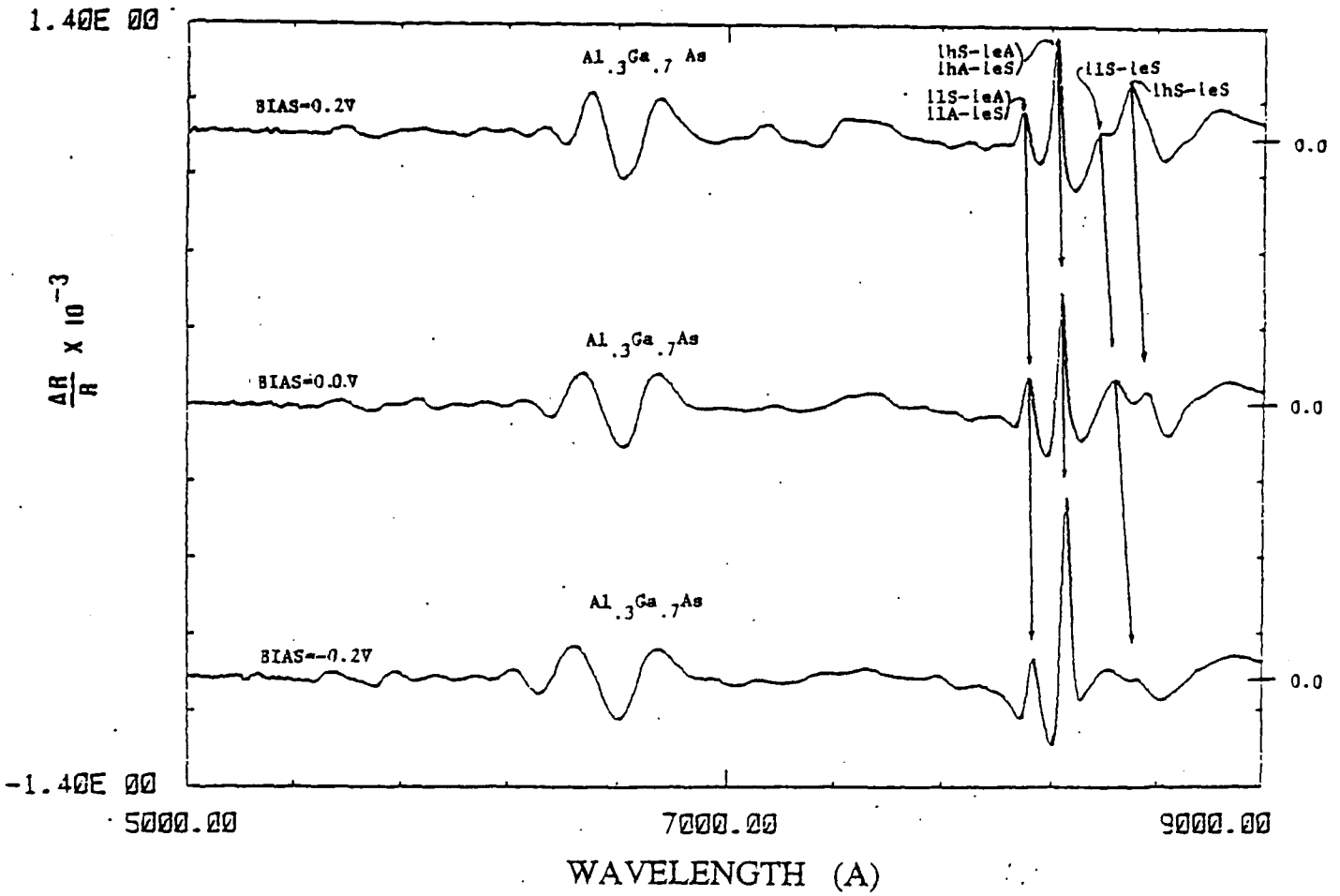

Fig. 7 Electroreflectance spectra on a 20-5-20 monolayer CDQW single pair at room temperature for 0.2V (forward bias), 0.0V, and -0.2V (reverse bias). The total thickness of the CDQW region is 1153 A. The zero level of each spectrum has been offset.

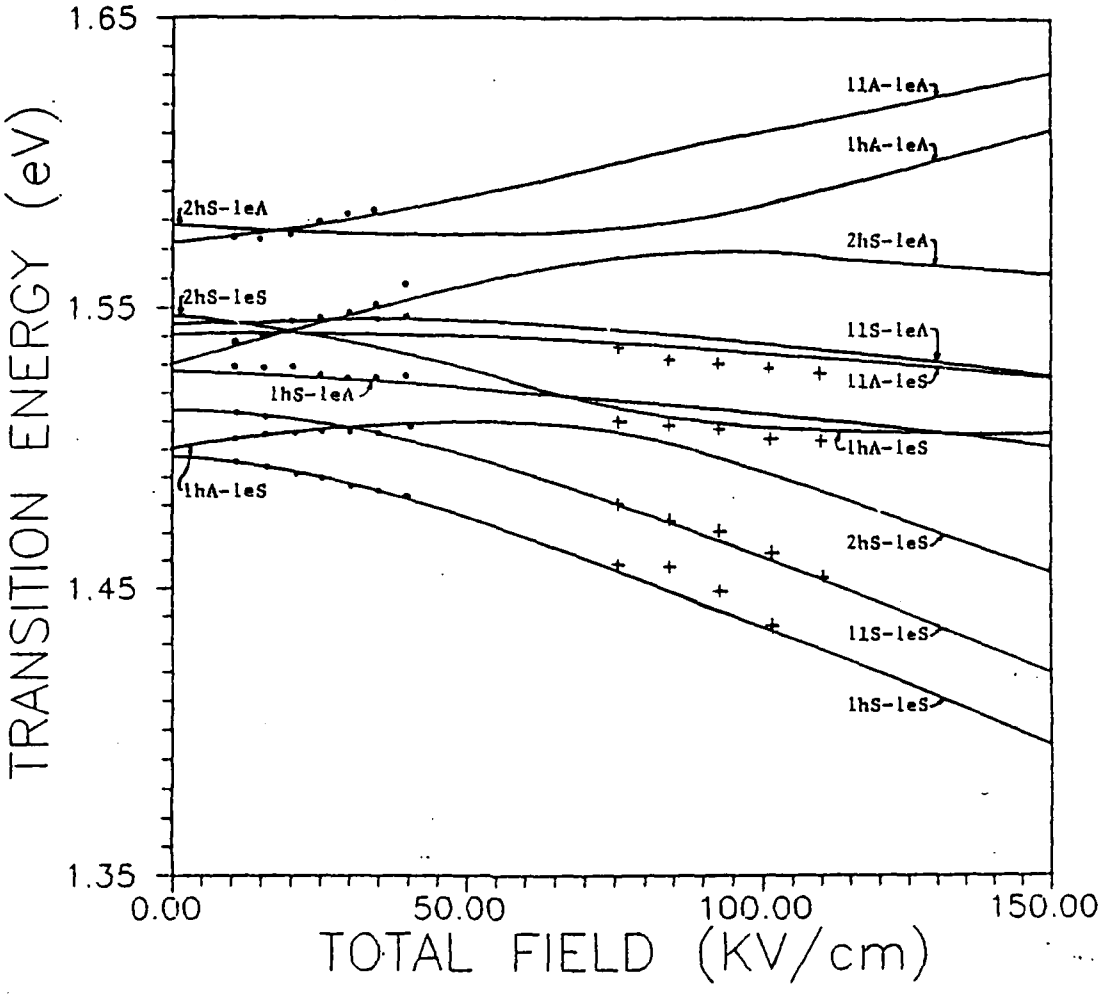

Fig. 8 Calculated (solid line) and measured photocurrent ( ) and electroreflectance (+) transition energies as a function of total field for a 20-5-20 monolayer CDQW is shown. The nomenclature of the assigned peaks are in the text.

(I.E) LASER ASSISTED AND NON-ASSISTED MBE GROWN GaAs on Si(100):

The system GaAs on Si is of interest for its significance to integration of optoelectronic devices with Si devices and circuitry. The fundamental materials growth and Physics issues that are impeding the progress, however, arise from the lattice mismatch (4% compressive), thermal expansion mismatch, and bonding aspects of a heteropolar material on homopolar substrate. We undertook to examine the optical properties (and structural properties under separate sponsorship by ONR) of THIN (<0.3 m) GaAs films grown on Si(100) substrates, offcut 4° towards [110], via **MBE UNDER EXCIMER LASER IRRADIATION** to influence the growth kinetics. The growth was carried out under ONR sponsorship. The *KrF 248 nm line was used* and the irradiation angle and beam (unfocussed) diameter are such that on the 2" Si wafer only a central ellipse with major and minor axes of 1.5 cm and 1 cm, respectively, is the laser-assisted growth area. Thus, on the same sample we can examine laser assisted and non-laser (i.e. usual) assisted growth regions for a comparative study of the optical and structural properties.

The optical properties were examined under the present grant employing PL, Raman scattering, and Rayleigh scattering. In fig. 9 are shown the 4K PL spectra from the laser assisted (panel a) and non-laser assisted regions. Note that both regions show significant near edge luminescence (bulk GaAs excitonic luminescence being at 1.579 eV) which is at least two orders of magnitude higher than previous reports for even thick GaAs films

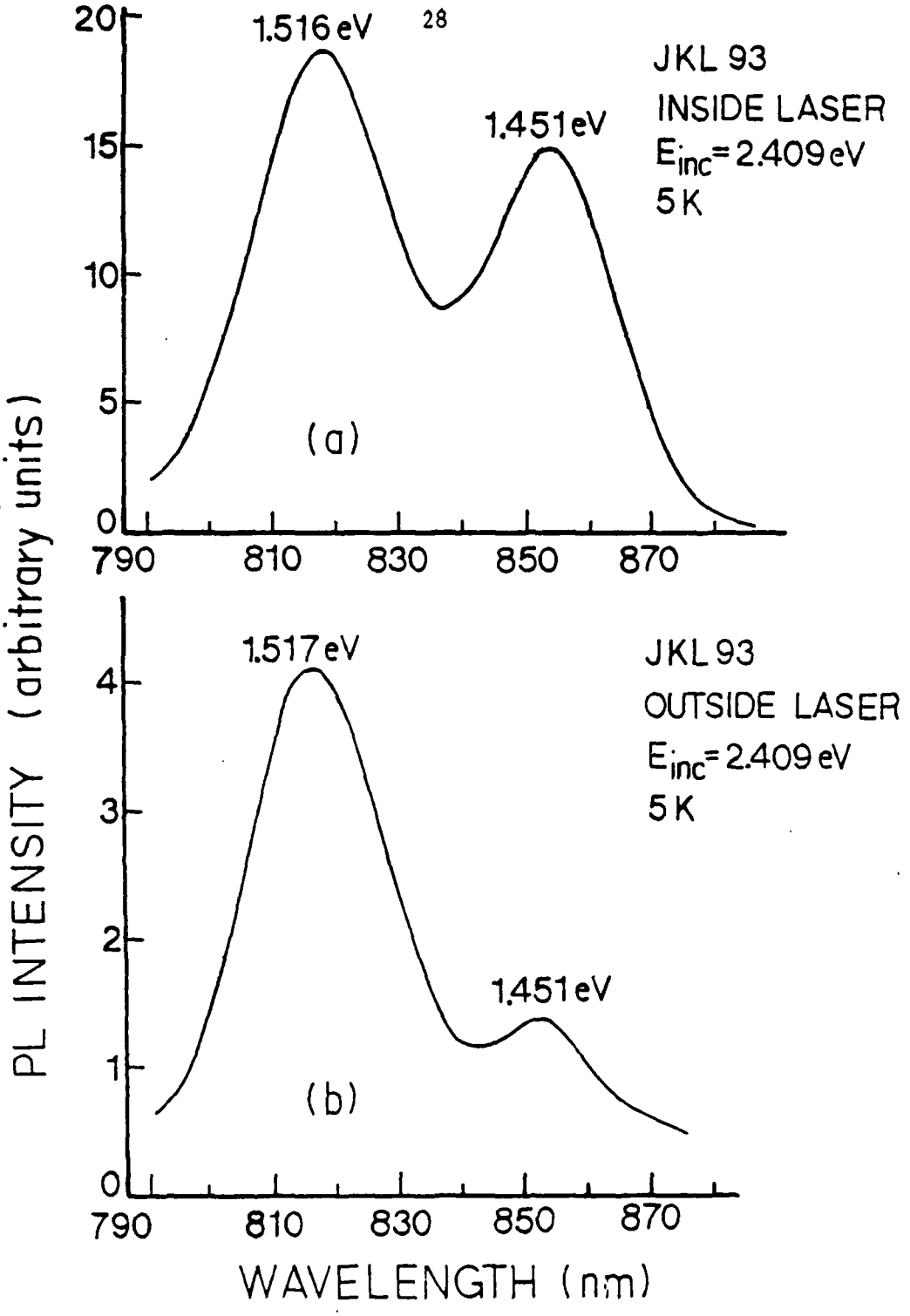
1.516 eV
1.451 eV
JKL 93
INSIDE LASER
E_{inc} = 2.409 eV
5 K
(a)
1.517 eV
1.451 eV
JKL 93
OUTSIDE LASER
E_{inc} = 2.409 eV
5 K
(b)
PL INTENSITY (arbitrary units)
WAVELENGTH (nm)
790
810
830
850
870

Fig. 9

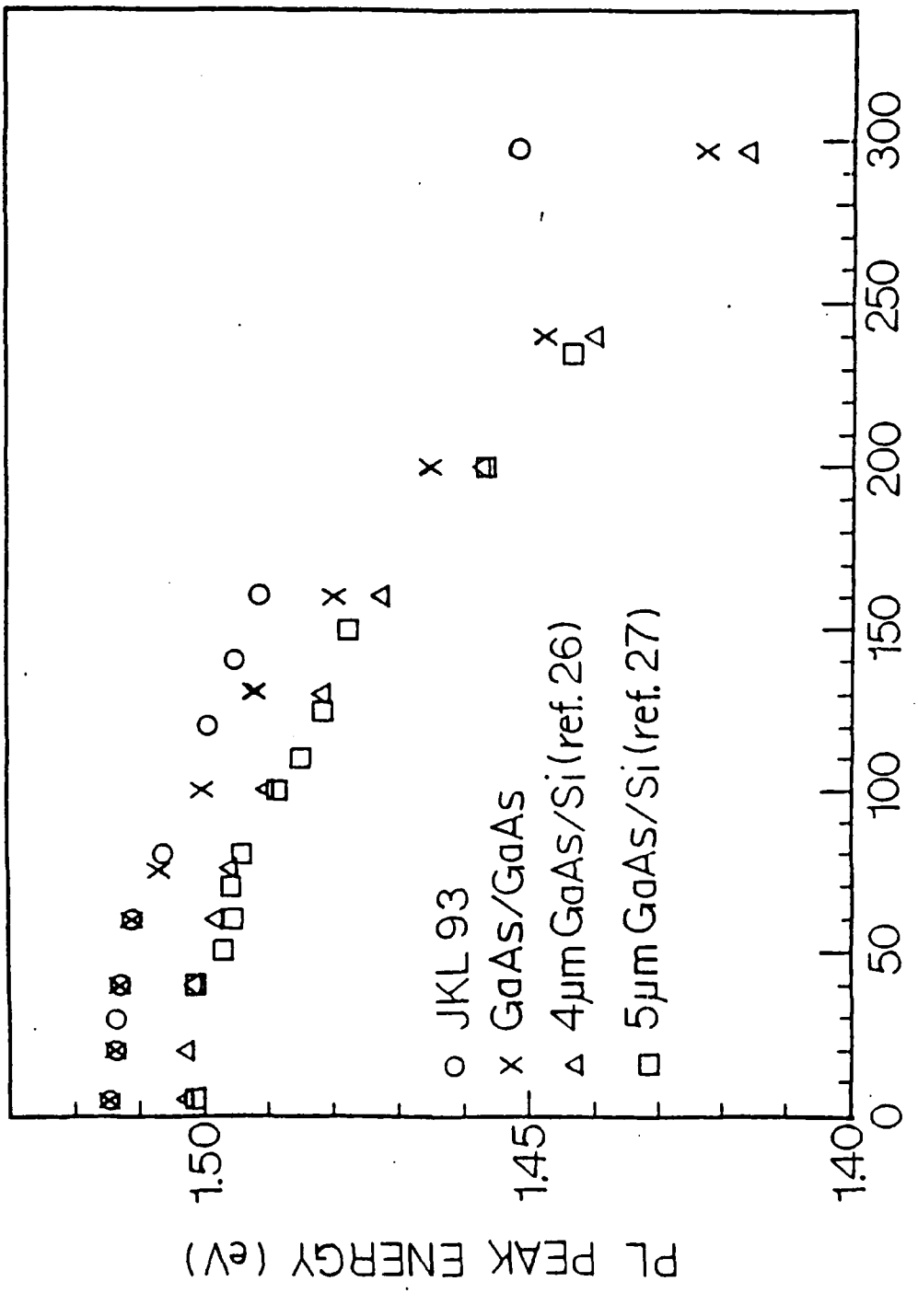
PL PEAK ENERGY (eV)
1.50
1.45
1.40
0
50
100
150
200
250
300
TEMPERATURE (K)
o JKL 93
x GaAs/GaAs
Δ 4μm GaAs/Si (ref. 26)
□ 5μm GaAs/Si (ref. 27)

FIGURE 10

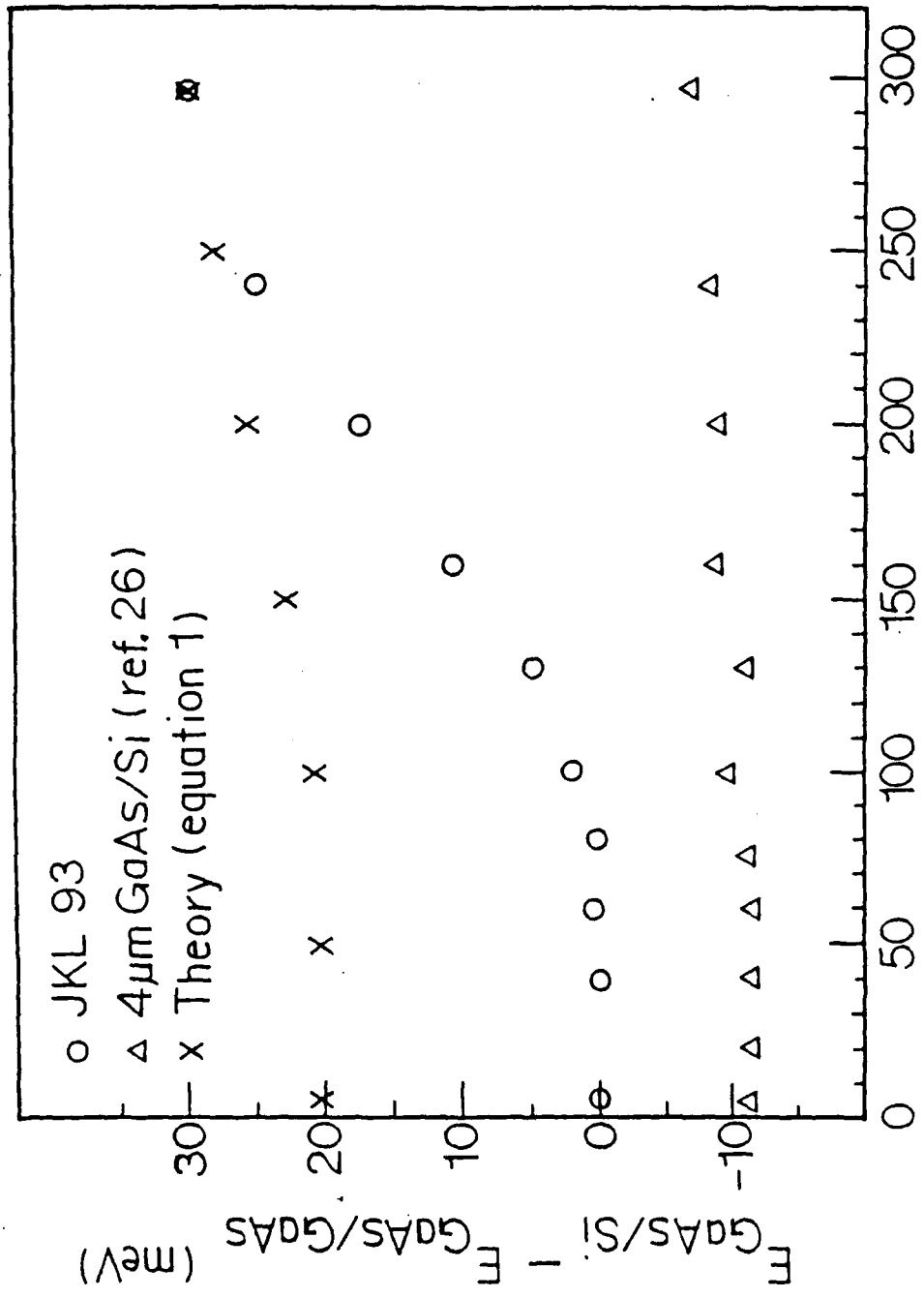
o JKL 93
Δ 4μm GaAs/Si (ref. 26)
x Theory (equation 1)
30
20
10
0
-10
0
50
100
150
200
250
300
TEMPERATURE (K)
$E_{GaAs/Si} - E_{GaAs/GaAs}$ (meV)

Fig. 11

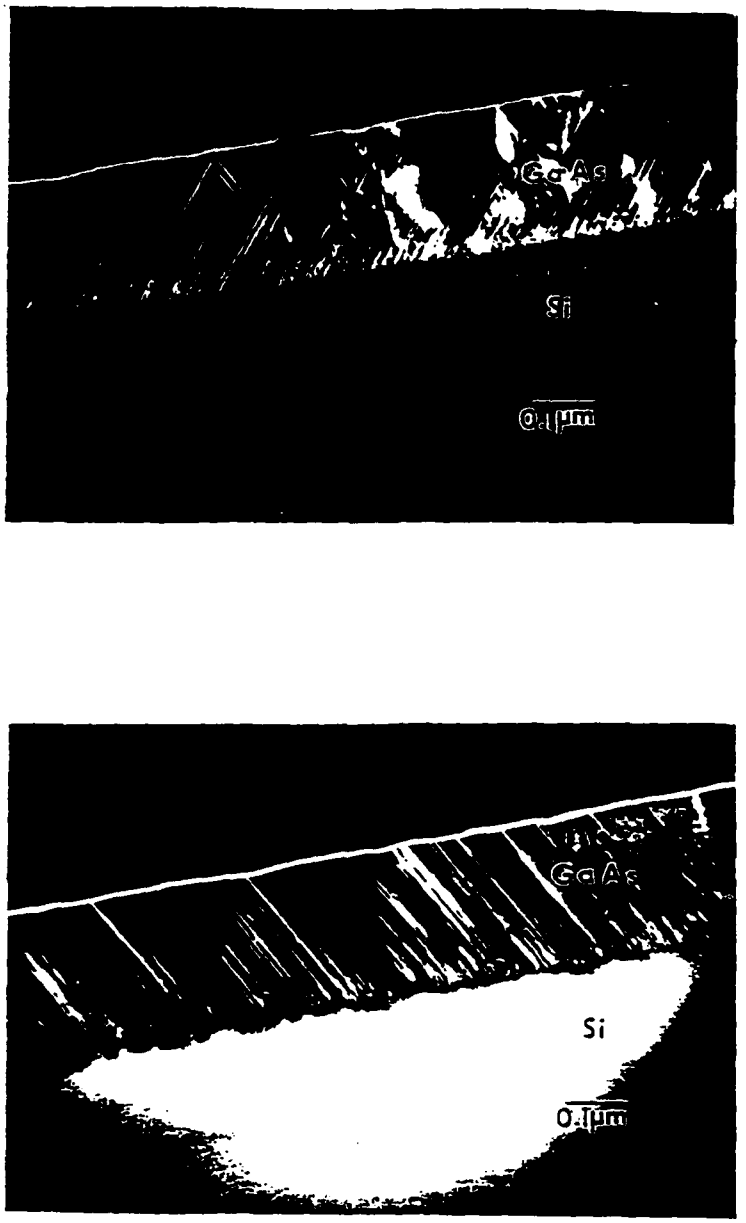

Fig. 12. Shows cross-sectional TEM Dark Field images of the two twin variants in thin (2800 A) GaAs film on Si (100) cut 4° towards [110]. Note that one type of twin reaches the surface more so than the other.

on Si. In addition, the luminescence from the laser assisted area is about a factor of 5 higher than the non-laser area, although a factor of two enhancement is a consequence of a higher film thickness. Consequently, a factor of 2 enhancement in the PL intensity from the laser area is extracted from the new data. In fig. 10 and fig. 11 are shown, respectively, the temperature dependence of the PL emission peak energy and of the separation of the peak from bulk GaAs emission line. For comparison are also shown previously reported data for thick (>1μm) GaAs films grown on Si. Though the data in figs. 10 and 11 are for the laser-assisted area, the non-laser assisted area show precisely the same values. The significant and new finding here is that figs. 10 and 11 reveal the presence of residual compressive strain in the thin film even though its thickness is more than an order of magnitude higher than predicted by the usually employed thermodynamic ground state theories. Thus the misfit dislocations present do not cause complete relaxation of the compressive strain.

Though not a part of the study undertaken under the present ARO grant, in fig. 12 we show cross sectional TEM micrographs of the laser-irradiated region which shed light on the above noted inferences derived from the optical studies. The two micrographs are taken to show the existence of two types of twins of which one type dominates the surface region. We have identified this twin variant to correspond to twins that are oriented in a direction away from the step edges of the vicinal Si(100) substrate and provided energy consideration arguments to explain their origin.

This is also the first time the existence of the two twin variants, their orientational relationship to the step edges of the vicinal substrates commonly employed (to reduce the density of antiphase domain boundaries), and an explanation of their origin has been shown. Further details may be found in publication nos 14 and 18.

(I.F) PHOTOLUMINESCENCE FROM WELLS GROWN ON PATTERNED SUBSTRATES:

Patterning of grown quantum well structures is almost invariably done to create an array of discrete devices. In recent times, such patterning is often done employing electron beam lithography motivated by the desire to create device dimensions near 0.1 μm or, from a basic physics study perspective, to create nanostructures for examination of electrical and optical properties of structures having 2 degrees of confinement (QUANTUM WIRES) or 3 degrees of confinement (QUANTUM BOXES or DOTS). An alternative to post-growth patterning, however, is to pattern the starting substrate and then grow the desired combination of ultra-thin layers. This is a particularly desirable goal for nanostructures since it affords the possibility of reducing many processing-step related introduction of defects, contaminants, etc. and, if done via a direct-write patterning technique, is compatible with in-situ patterning in an ultra-pure environment and direct transfer to the growth chamber. For an MBE system this would be a UHV environment throughout.

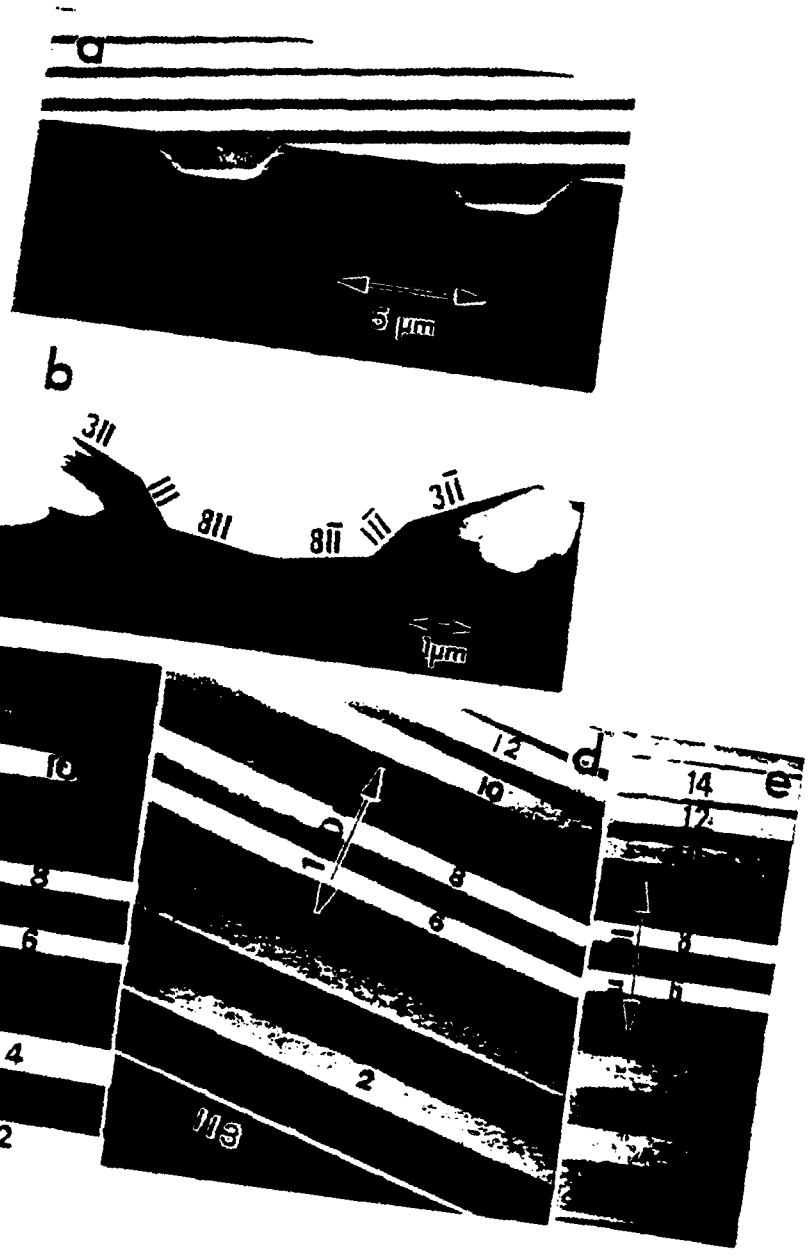
a
5 μm
b
3̄11
111
8̄11
8̄1̄1
1̄11
3̄1̄1
1μm
c
10
8
6
4
2
d
12
10
8
6
2
113
e
14
12
8
6

Fig. 13

Under the present ARO grant we have undertaken optical studies of GaAs/$Al_xGa_{1-x}As$ quantum well structures grown in our MBE systems on GaAs(100) substrates patterned ex-situ via optical lithography. The growth per se is supported by the AFOSR. Although ex-situ optical patterning available to us at USC places a lower limit of 1 μm on the dimensions of the as-patterned features (grooves, mesas, etc.), an illustrative example of a set of parallel grooves running along the [ITO] direction being shown in the SEM picture of fig. 13(a), we have, through exploitation of growth kinetics, developed a way of creating structures down to 1000A feature size. This aspect relates to the thrust of the research proposed in the next section and we shall return to it momen-tarily. First we provide a very brief report on the formation of quantum well structures with lateral dimensions > 2 μm.

In fig. 13(b) is shown a cross sectional TEM low magnification view of the profile GaAs/$Al_xGa_{1-x}As$ multilayered structure has been grown on the patterned substrate of panel (a). Note the presence of facets such as (311) between the starting (111) side wall and the top (100) terrace, and (811) between the (111) side wall and the trench botton (100) plane. In panel (d) is shown the dark-field image contrast of the trench bottom and side wall region, the lighter layers being AlGaAs. The layers defining the quantum wells on the side walls are significantly thinner than expected on the basis of the incident flux whereas the layers defining the QW's on the trench bottom are significantly thicker. This is a consequence of the inter-facet

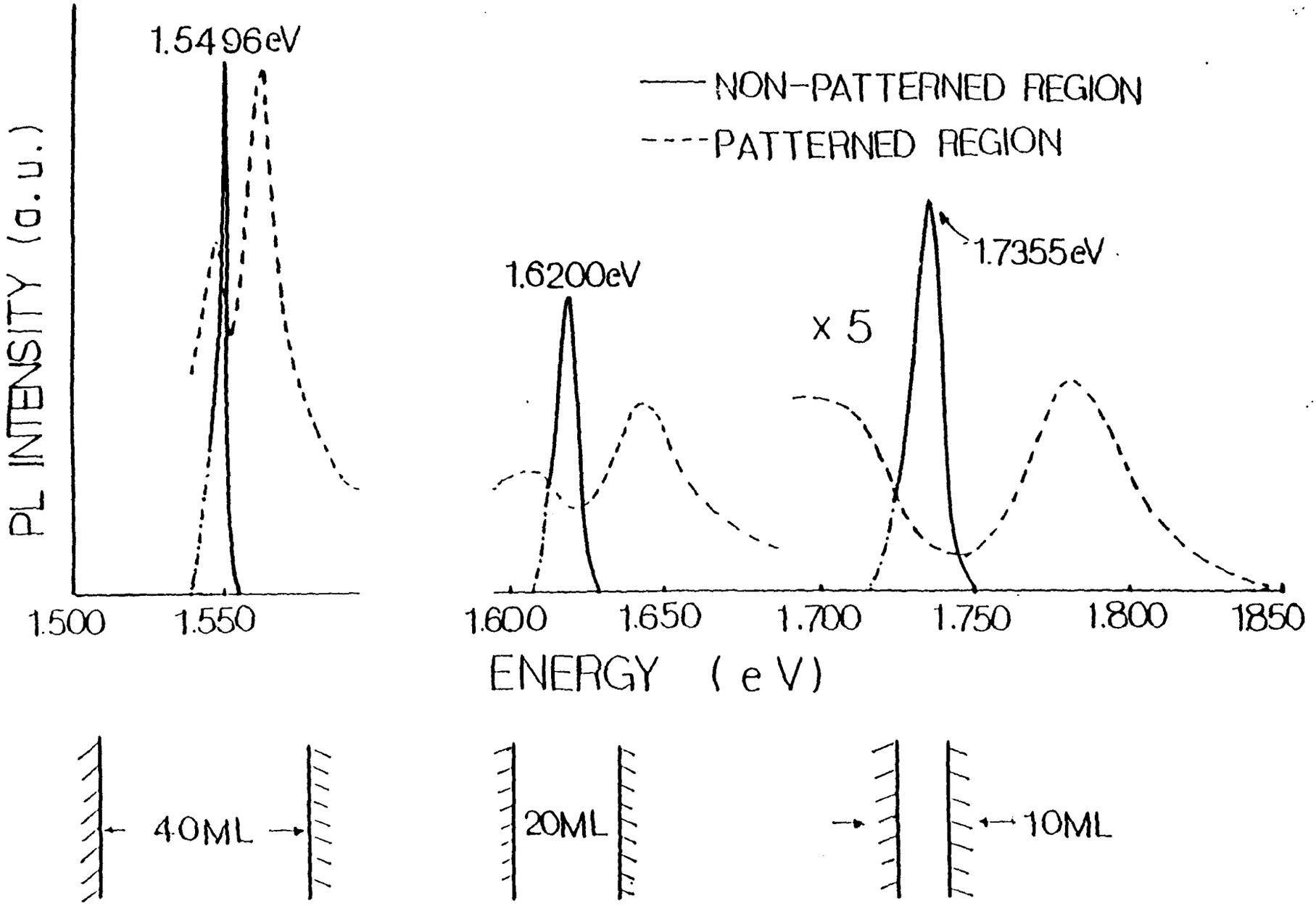
1.5496eV
NON-PATTERNED REGION
PATTERNED REGION
PL INTENSITY (a.u.)
1.6200eV
1.7355eV
x 5
1.500
1.550
1.600
1.650
1.700
1.750
1.800
1850
ENERGY (eV)
40ML
20ML
10ML

Fig. 14

migration from the side walls to the trench bottom, a phenomenon observed in the very first studies[4] by Tsang and Cho over a decade ago. In recent times this has been exploited[5,6] to create laterally confined laser structures by exploiting the mismatch in the confined electronic states of the side wall QW's and the trench bottom QW's. In panel (c) is shown the QW's formed on the (311) facet. Note that, as expected from the incident flux relationship between (311), (111) and (100), the layer thicknesses in this case are intermediate between those on the (111) and (100) trench bottom. Finally, note the sharpness of the interfaces on the (311) and (100) trench bottom, indicating fairly high quality MQW formation. Panel (e) of fig. 13 shows the layer thickness in a *non-patterned part of the same* substrate and provides an unambiguous reference for measuring deviations in thicknesses of the layers on different facets in the patterned region.

We have examined the photoluminescence behavior of QW's grown on a variety of patterned substrates with varying groove dimensions and widths of the top (100) terrace. An illustrative result, taken on the sample of fig. 13, is shown in fig. 14. The solid curves are the PL emission from the non-patterned region and provide a marker for the optical behavior. The broken line curves show the PL emission from the uppermost three quantum wells of thickness 10 ML, 20 ML, and 40 ML in the non-patterned region. Note that each of the single line emission of the non-patterned region shows at least two peaks, one at a lower and the other at a higher energy. This is consistent with the higher than reference

thickness for the QW's formed at the trench bottom (100) face and lower than reference thickness for the QW's formed on the (311) and (111) facets. The measured peak positions of the doublets do not exactly coincide with those calculated on the basis of the change in the GaAs well layer thickness alone. This we believe is as should be expected on the basis of the growth kinetics, the difference in the Ga and Al interfacet migration kinetics leading to a difference in the Al concentration of the trench bottom alloy barrier layers as compared to the ones on the side facets - lower overall Al concentration for the former and higher overall Al concentration for rhe latter. In addition, a fundamental feature never established in the literature but often assumed is the orientation dependence of the band edge discontinuity. There is no a priori reason to assume that the near 60:40 split in the band gap difference for conduction and valence bands now well tested for the (100) orientation GaAs/$Al_xGa_{1-x}As$ is also necessarily true for other orientations such as the (311) and (111) orientations involved here. Thus the precise depth of the QW potential on different facets remains uncertain. Indeed, in section IV on proposed research we propose to establish these fundamental relations via a combination of optical and electrical studies of QW's grown on non-patterned substrates of such orientations (i.e. (111), (311), etc.).

(I.G) QUANTUM WIRE STRUCTURE:

Finally, in fig. 15 we show an example of a remarkable way of

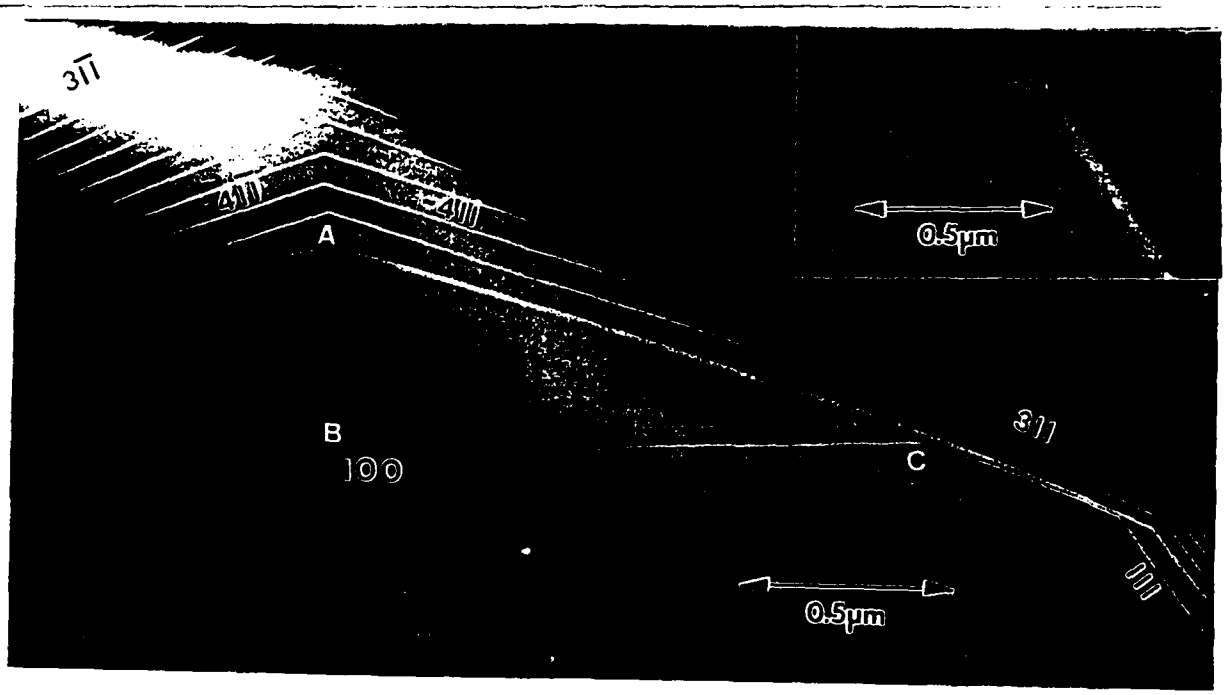

Fig. 15

exploiting growth kinetics for in-situ creation of quantum wires and quantum dots, even though patterning may be done ex-situ and on length scales of > 1 m. Under appropriate growth conditions, the starting sharp edge between the top (100) terrace and the (111) side wall of the as-patterned substrate (shown in the inset) gives rise to the formation of a (311) transition facet immediately after thermal desorption of the native oxide prior to growth initiation. This is clearly seen in the main figure where the very first light colored "line" corresponds to 10 ML AlAs layer grown as a marker to define the starting profile of the substrate after oxide desorption. Note that during subsequent deposition of GaAs, no growth occurs on the (311) facet so long as the top(100) terrace remains adjacent. The $Al_{0.4}Ga_{0.6}As$ marker layer numbered 2 not only clearly demonstrates this behavior, but also then shows that the truncated pyramidal profile of the GaAs growing on the top (100) terrace provides a (100) "substrate" of smaller and smaller lateral dimension with growth. The lateral dimension defined by the marker layer 2 in the region labelled A in fig. 15 is about 2000 A. Subsequent growth of GaAs and deposition of the $Al_{0.4}Ga_{0.6}As$ layer labelled 3 then creates, in-situ, a pyramidal shaped quantum wire structure. This is a powerful way of creating nanostructures for a variety of basic optical and electrical studies for it avoids a number of contamination and damage issues faced with in techniques employing patterning on the scale of the desired nanostructure. It also has the great practical advantage that it makes possible creation of

at least certain types of nanostructures without the need for elaborate and expensive ex-situ or in-situ patterning and processing techniques (such as electron beam lithography and focussed ion beam induced impurity disordering being employed in the few attempts at producing nanostructures reported so far).

Work on the optical properties of structures grown on patterned substrates is presently continuing. We are, however, faced with the need for a spatially resolved optical technique for certain aspects of this work. We have made arrangements with Dr. M. Dutta of US ARMY Laboratory at Ft. Monmouth to carry out, collaboratively, Micro-Raman studies at such facilities available in her laboratory.

II. WORK IN PROGRESS:

Work is presently continuing on several projects not all of which have been covered in the preceding sections. Here we provide a brief report of the objective and status of these projects.

(II.A) VERTICAL TRANSPORT:

Electron transport across interfaces offers several interesting studies of tunnelling phenomenon as well as the potential for new types of devices. In particular, resonant tunnelling has attracted considerable interest in the past few years - both in the context of the basic physics underlying the

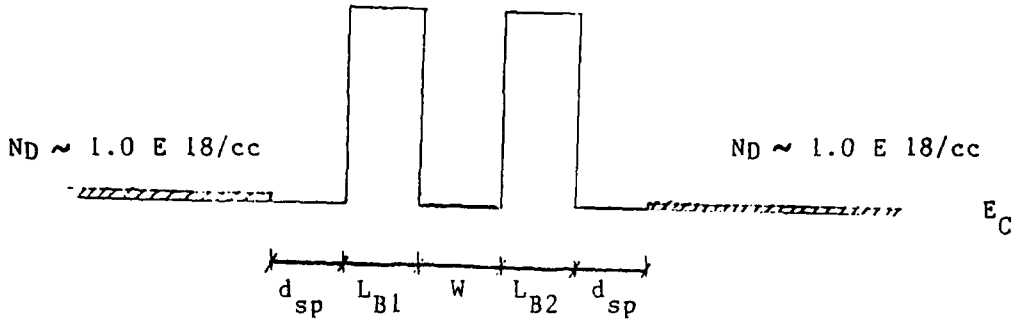

Figure 16a Schematic of Resonant Tunneling Diode conduction band profile. The spacers and well are undoped GaAs while the barriers are undoped $Al_xGa_{1-x}As$.

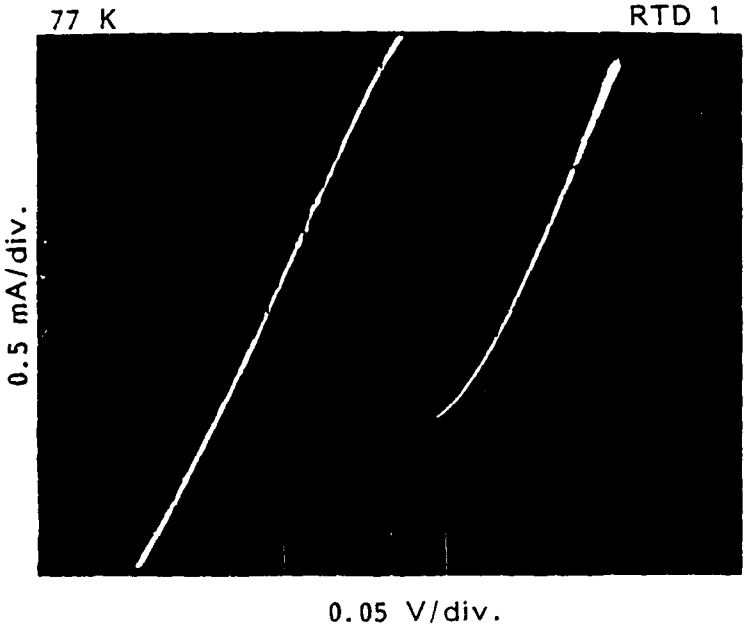

Figure 16b I-V curve of RTD 1 having 30% Al barriers measured at 77 K. The device dimension is 12 x 12 um. This device shows a Peak to Valley Ratio of 3.3 with a peak current density of 3.5 kA/cm^2. Note that origin of I-V curve is shifted to bottom of third quadrant.

process and the potential of extremely fast devices. Our interest in resonant tunnelling arises from both these context with particular interest in exploring ways of achieving high peak currents (~ 10 KAmp/Cm^2) and peak-to-valley ratio (>10) through growth of appropriate materials. We initiated our studies through growth of GaAs/$Al_xGa_{1-x}As$(100) resonant tunnelling diodes with the objective of eventually moving towards the GaAs/(InAs/AlAs) material system.

We have grown and processed several GaAs/$Al_xGa_{1-x}As$ resonant tunnelling diodes. The generic structure (fig. 16a) consists of a 1 m thick Si-doped (N_D-1E18/cc) GaAs buffer grown on top of a n^+ GaAs substrate, 18 monolayer (ML) undoped GaAs spacer, two 18 ML undoped $Al_xGa_{1-x}As$ barriers with a 20 ML undoped GaAs well sandwiched between them, 18 ML undoped GaAs top spacer and a 0.6 m n^+ Si-doped (N_D-1E18/cc) GaAs cap layer. Samples with barrier composition x=0.3, 0.5, 1.0 have been grown for the purpose of studying the effect of different barrier heights, and the effects of direct-to-indirect gap barrier on the peak to valley ratio (PVR) and the peak current density of the negative differential resistance (NDR) feature in I-V characteristics of the device. All of these samples were grown dynamically (i.e. without any growth interruption at heterointerfaces). A sample with x=0.3 was grown with growth interruption at the heterointerfaces to compare with its counterpart. All of the above samples were processed into 100 μm x 100 μm and 12 μm x 12 μm square mesas with alloyed AuGe/Ni/Au Ohmic contacts on top and a large area alloyed In

contact at the bottom of the chip serving as the bottom contact. Devices processed from all of the samples show NDR at a temperature of 77K as well as 300K. A representative I-V curve is shown in rigure 16(b) for x_{Al}=0.3, non-interrupted growth. A PVR of 3.3:1 at 77K with a peak current density of 3.5 KA/Cm^2. This high peak current density for x_{Al}=0.3 is among the best reported in the literature. The I-V curve shows hysteresis due to extrinsic effects such as lead resistances, as well as due to the intrinsic phenomenon of well charging. These effects are currently being investigated.

(II.B) MAGNETO-QUANTUM-TRANSPORT:

The discovery of the integral quantum Hall effect[7] (IQHE) and the fractional quantum Hall effect[8] (FQHE) has lead to extensive experimental and theoretical investigations of both these phenomena[7,8]. Most of these studies, particularly of FQHE, have been carried out on the GaAs/$Al_{0.3}Ga_{0.7}As$(100) heterojunction (HJ) system which offers high low temperature mobilities (as high as $5x10^6$ at 4.2K) for electron density of $3\text{-}5x10^{11}$/Cm^2. To achieve the FQHE regime (Landau level filling factors, $\nu < 1$) at these densities requires magnetic fields in excess of ~14T, $\nu = 1/3$ being reached at a field ~42T. To achieve both odd-denominator and even-denominator values in the FQHE regime at easily accessible magnetic fields in ordinary laboratories, it is desirable to achieve electron densities of $1\text{-}3x10^{10}$/Cm^2 without compromising the low temperature mobility too much. At such densities in the

$GaAs/Al_{0.3}Ga_{0.7}As(100)$ HJ system $\nu=1$ is reached at ~1.5T. Equally significant, with fields as high as 60T available at a few National Laboratories, such a system would permit reaching values as small as (1/40). At these low values and low temperatures (mk regime) it is predicted[9] that the quantum Wigner solid should be realizable, as opposed to the highly correlated quantum fluid states underlying the FQHE regime[10].

Motivated by an interest in the Physics of this regime, we undertook the realization of high mobilities at carrier densities in the $1\text{-}3x10^{10}/Cm^2$ regime. As noted in sec. (I.A), we have successfully grown $GaAs/Al_{0.25}Ga_{0.75}As(100)$ inverted HEMT structures with carrier concentration $3x10^{10}/Cm^2$ and LN_2 (Dark) mobilities of 145,000 $Cm^2/VSec$. The LH_e mobilities are 3-4 x $10^5 Cm^2/VSec$. These samples are ideally suited for the studies noted above.

Work on making Hall-bar geometries and placing appropriate Ohmic contacts has been underway. Lack of appropriate facilities for achieving such a task at USC has kept progress on this front slow and, given the enthusiasm for finally having the chance to examine the exciting Physics that lies ahead, also created a sense of frustration. Nevertheless, we are finally beginning to overcome this road block and expect to be in a position to undertake these studies very shortly. In the meantime, with the standard Van der Pauw geometry (quite unsuited for the physics measurements of interest) we have carried out some measurements, including measurements carried out up to about 30T at the High

Magnetic Field facility of Institut National des Sciences Appliquees (INSA), Toulouse (France) in collaboration with Prof. J. Leotin and his students. We anxiously look forward to carrying out these measurements with the appropriate Hall-bar geometry samples up to the 60T field available at INSA (Toulouse), following studies up to 7T available in our own laboratory at USC.

(II.C) CYCLOTRON RESONANCE:

In collaboration with Prof. J. Leotin of INSA (Toulouse), we are presently engaged in carrying out far infrared cyclotron resonance (CR) measurements on the high mobility I-HEMT's (including the special structure with the very low carrier concentrations of $2\text{-}4\times10^{10}/Cm^2$) and on the single-side doped single square quantum well (SSQW) structures discussed in sec. (I.A). On the SSQW structures the CR measurements shall serve as an independent test of the unique feature of the inverted SSQW we delineated in sec. (I.A) - namely, the influence of the inverted interface quality on the mobility revealed through the rise in the I-SSQW mobility as compared to the I-HEMT.

(II.D) ABSORPTION IN COUPLED-DOUBLE QUANTUM WELLS:

The variety of optical studies of the CDQW structures discussed in sec. (I.D), including the effect of externally applied bias to examine the potential of such structures for amplitude or phase modulation based SLM's, have lacked one very basic and complimentary measurement - absorption in a transmission

geometry. Such measurements are particularly important for minimizing ambiguities in comparison with calculations caused by uncertainty in precisely determining the built-in electrostatic field arising from unintentional doping and defects. We have been limited in our ability to carry out such measurements for they require very controlled etching of the absorbing GaAs substrate. Even though the structures are grown with an appropriate etch stop layer, such a task requires very careful and controlled etching with high accuracy so as not to make the QW active structure (~1 μm thick) mechanically vulnerable. Lack of access to such etching facilities prevented us through most of 1988 from undertaking these measurements. However, recently a Jet Thinning Apparatus has been made available to us by our colleague, Prof. P.D. Dapkus (USC), and we are presently in the midst of making a few appropriate modifications to this system to make it suitable for our objective. We thus expect very shortly to begin absorption measurements on the wide range of CDQW structures we have systematically examined via PL, PLE, ER, PR and PC measurements since Fall '87.

REFERENCES:

1. A. Ourzmad, paper presented at the MRS Fall Meeting, (Boston, Ma.) Dec. 1988.

2. A. Madhukar and S. Das Sarma, Surf. Sc. 98, 135 (1980); S. Das Sarma and A. Madhukar, Phys. Rev. B22, 2823 (1980).

3. D.A. B. Miller, D.S. Chemla, T.C. Damen, T.H. Wood, C.A. Burras Jr., A.C. Gossard and W. Weigmann, IEEE Jour. Quantum Elec. QE-21, 1462 (1985) and references therein.

4. W.T. Tsang and A.Y.Cho, App. Phys. Letts. 30, 293 (1977).

5. E. Kapon, M.C. Tamargo and D.M. Hwang, App. Phys. Lett. 50, 347 (1987).

6. E. Kapon, C.P. Yun, D.M. Hwang, M.C. Tamargo, J.P. Harbison and R. Bhat, Proceedings of the SPIE Symposium on "Growth of Advanced Compound Semiconductor Structures, Editor A. Madhukar, Vol.944, p.80 (1988).

7. See, for example, K. von Klitzing, Rev. Mod. Phys. 58, 519 (1986) and references to earlier work therein.

8. For a good review of FQHE, see H. Stormer, Lecture Notes in Proceedings of the NATO Advanced Summer School on Two Dimensional Systems (Banff, Canada, Sept. 1987), Plenum Press (N.Y.).

9. P.K. Lam and S.M. Girvin, Phys. Rev. B30, 473 (1984).

10. R.B. Laughlin, Phys. Rev. Letts. 50, 1395 (1983).

III. ARO SUPPORTED PUBLICATIONS:

1. S.B. Ogale, A. Madhukar, F. Voillot, M. Thomsen, W.C. Tang, T.C. Lee, J.Y. Kim and P. Chen, "Atomistic Nature of Heterointerfaces in III-V Semiconductor-Based Quantum-Well Structures and its Consequences for Photoluminescence Behavior", Phys. Rev. B36, 1662 (1987).

2. S.B. Ogale, A. Madhukar and N.M. Cho, "Photoluminescence Linewidth Systematics for Semiconductor Quantum Well Structures with Graded Interface Composition Profile", App. Phys. Letts. 63, 578 (1987).

3. S.B. Ogale, A. Madhukar and N.M. Cho, "Influence of Transverse Electric Field on the Photoluminescence Linewidth of Excitonic Transition in Quantum Wells: Alloy Disorder and Composition Fluctuation Contributions", J. Appl. Phys. 62, 1381 (1987).

4. A. Madhukar, P.D. Lao, W.C. Tang, M. Aidan and F. Voillot, "Observation of Phonon Modes through Resonant Mixing with Electronic States in the Secondary Emission Spectra of $GaAs/Al_{0.32}Ga_{0.68}As$ Single Quantum Well", Phys. Rev. Lett. 59, 1313 (1987).

5. N.M. Cho, S.B. Ogale and A. Madhukar, "Low Temperature Electron Transport in One-side-modulation-doped $Al_{0.33}Ga_{0.67}As/GaAs/ Al_{0.33}Ga_{0.67}As$ Single Quantum Well Structure", Appl. Phys. Lett. 51, 1016 (1987).

6. N.M. Cho, S.B. Ogale and A. Madhukar, "Electron Transport in One-side-modulation-doped Single Quantum Well Structure: Remote Ion Scattering Contribution", Phys. Rev. B36, 6472 (1987).

7. P.D. Lao, W.C. Tang, A. Madhukar and F. Voillot, "Resonant Mixing between Electronic and Optical Vibrational States of a Quantum Well Structure", Jour. de Physique, 48, C5-121 (1987).

8. W.C. Tang, P.D. Lao, A. Madhukar and N.M. Cho, "A Combined Rayleigh and Raman scattering study of $Al_xGa_{1-x}As$ Grown via Molecular Beam Epitaxy Under Reflection High Energy Electron Diffraction Determined Growth Conditions", Appl. Phys. Lett. 52, 42 (1988).

9. Anupam Madhukar, "Exploiting Kinetics in Molecular Beam Epitaxial Growth for Realization of High Quality Normal and Inverted Interfaces", Workshop on HEMT, Organized by U.S. Army Electronics and Device Technology Laboratory, Ft. Monmouth, New Jersey, Jan, 27-28, 1988.

10. P.G. Newman, N.M.Cho, D.J.Kim, A.Madhukar, D.D.Smith, T.R.Aucoin and G.J.Iafrate, "Surface Kinetic Considerations for MBE Growth of High Quality Inverted Heterointerfaces", Proceedings of the 15th PCSI Conference, (Feb. 1-4, 1988; Asilomar, Ca.); Jour. Vac. Sc. Tech.B6, 1483 (1988).

11. N.M. Cho, P.G. Newman, D.J.Kim, A. Madhukar, D.D. Smith, T. Aucoin and G.J. Iafrate, "Realization of High Mobility in Inverted $Al_xGa_{1-x}As$/GaAs Heterojunctions", App. Phys. Lett. 52, 2037 (1988).

12. Pudong Lao, Wade C. Tang, A. Madhukar and P. Chen, "Alloy Disorder Effects in Molecular Beam Epitaxically Grown $Al_xGa_{1-x}As$ Examined Via Raman and Rayleigh Scattering and near Edge Luminescence", Proceedings of the SPIE Conference on "Advances in Semiconductors and Superconductors: Physics and Device Applications" (13-18 March, 1988, Newport Beach Mariott Hotel, CA), SPIE Vol. 946, p.150 (1988).

13. W.C. Tang, Pudong Lao, and A. Madhukar, "Optical Investigation of Resonant Mixing Between Electronic and Optical Vibrational Levels in GaAs/$Al_xGa_{1-x}As$ Single Quantum Wells", Proceedings of the SPIE Conference on "Advances in Semiconductors and Superconductors; Physics and Device Applications", (13-18 March, 1988, Newport Beach Mariott Hotel, CA), SPIE Vol. 943, p.170 (1988).

14. F.J. Grunthaner, A. Madhukar, J.K. Liu, W.C. Tang, P.D. Lao, S. Guha, P. Anderson, J. Ionelli and B. Pate, "Laser-assisted Molecular Beam Epitaxial Growth of GaAs on Si(100)", SPIE Proceedings, Vol. 944, 153 (1988).

15. Pudong Lao, Wade C. Tang, A. Madhukar and P. Chen, "A Combined Single Phonon Raman and Photoluminescence Study of Direct and Indirect Band Gap $Al_xGa_{1-x}As$ Alloys Grown by Molecular Beam Epitaxy", Jour. Appl. Phys. 65, 1676 (1989).

16. S. Guha, A. Madhukar, K. Kaviani, Shizhong Xie, M. Hyugaji, Ravi Kuchibhotla and Li Chen, "Inter-facet migration in Molecular Beam Epitaxy of $Al_xGa_{1-x}As$ on non-planar Patterned GaAs (001) Substrate", App. Phys. Lett. (Submitted).

17. D.J. Kim and A. Madhukar "Electron Hall Mobilities in Normal and Inverted Modulation Doped GaAs/AlGaAs Triangular and Square Quantum Wells", App. Phys. Letts. (Submitted).

18. P.D. Lao, W.C. Tang, K.C. Rajkumar, S. Guha, A. Madhukar, J.K. Liu and F.J. Grunthaner, Jour. App. Phys. (Submitted).

CONFERENCE PRESENTATIONS:

1. P.D. Lao, W.C. Tang, A. Madhukar and F. Voillot, "Resonant Mixing between Electronic and Optical Vibrational States of a Quantum Well Structure", 3rd International Conference on Modulated Semiconductor Structures (July 1987, Montpelier, France).

2. F.J. Grunthaner, A. Madhukar, J.K. Liu, W.C. Tang, P.D. Lao, S. Guha, P. Anderson, J. Ionelli and B. Pate, "Laser-assisted Molecular Beam Epitaxial Growth of GaAs on Si(100)", 15th PCSI Conference, (Feb. 1-4, 1988; Asilomar, Ca.).

3. Pudong Lao, Wade C. Tang, A. Madhukar and P. Chen, "Alloy Disorder Effects in Molecular Beam Epitaxically Grown $Al_xGa_{1-x}As$ Examined Via Raman and Rayleigh Scattering and near Edge Luminescence", SPIE Conference on "Advances in Semiconductors and Superconductors: Physics and Device Applications" (13-18 March, 1988, Newport Beach Mariott Hotel, CA).

4. W.C. Tang, Pudong Lao, and A. Madhukar, "Optical Investigation of Resonant Mixing Between Electronic and Optical Vibrational Levels in $GaAs/Al_xGa_{1-x}As$ Single Quantum Wells", *SPIE Conference on* "Advances in Semiconductors and Superconductors; Physics and Device Applications", (13-18 March, 1988, Newport Beach Mariott Hotel, CA).

IV. STUDENTS/POST-DOCS TRAINED:

1.	Mr. Nam-Min Cho	(Ph.D. 1988)
2.	Mr. Roger Kuroda	(Ph.D. Expected 1990)
3.	Mr. Do-Jin Kim	(Ph.D. Expected 1989)
4.	Mr. Wade C. Tang	(Ph.D. Expected 1989)
5.	Dr. P.D. LAO	(July '86 - Aug. '88)
6.	Dr. S. Xie	(Jan. '88 - Dec. '88).

V COLLABORATIONS/INTERACTIONS:

During the course of the activities undertaken under the present ARO grant a number of fruitful collaborations/interactions with colleagues at USC and other institutions have emerged. These collaborations serve the purpose of bringing complimentary expertise and/or facilities to bear upon issues of mutual interest and thus leverage each other's resources and investments. The dominant collaborations/interactions, which are to continue at an even higher level are with;

1. Profs. A.R. Tanguay Jr. and K. Jenkins (USC):

   Collaborative work on realization of 2D arrays of SLM structures for implementation of neural network models. Prof. Jenkins provides the systems perspective and Prof. Tanguay device processing and testing efforts.

2. Drs. D.D. Smith, M. Cole and M. Dutta (U.S. Army Electronic and Devices Laboratory, Ft. Monmouth, N.J.):

   The collaborative efforts here which bring complimentary expertise and resources to bear upon problems of common interest are;

   (a) Magneto-quantum transport (Dr. D.D. Smith)

   (b) High Resolution Electron Microscopy, including image simulation (Dr. M. Cole)

   (c) Micro-Raman Scattering (Dr. M. Dutta)

   studies of the proposed laterally confined structures.

3. Prof. J. Leotin (INSA, Toulouse, France):

   Collaborative work with Prof. Leotin utilizing the high

magnetic field (up to 60 T) and far infrared cyclotron resonance facilities shall continue on the laterally confined structures.

4. Prof. F. Voillot (INSA, Toulouse, France):

Time resolved photoluminescence studies (on the scale of ~ 7 pSec) of the laterally confined and nonconfined structures are underway in Prof. Voillot's laboratory and shall provide invaluable complimentary information to the time integrated optical studies undertaken at the principal investigator's laboratory at USC.